(1)

Low Temperature Photoluminescence Study Of Uranium Implanted into III-V Semiconductors and AlGaAs

THESIS

Michael B. Scott
Captain, USAF

AFIT/GEP/~~89D~~ ENP/89D-9

DEPARTMENT OF THE AIR FORCE
AIR UNIVERSITY
AIR FORCE INSTITUTE OF TECHNOLOGY

Wright-Patterson Air Force Base, Ohio

AFIT/GEP/89D-9

LOW TEMPERATURE PHOTOLUMINESCENCE STUDY OF URANIUM IMPLANTED INTO III-V SEMICONDUCTORS AND AlGaAs

THESIS

Presented to the Faculty of the School of Engineering

of the Air Force Institute of Technology

Air University

In Partial Fulfillment of the

Requirements for the Degree of

Master of Science in Engineering Physics

Michael B. Scott

Captain, USAF

December, 1989

Table of Contents

Acknowledgments

I would like to express my gratitude to my thesis advisor Dr. Y. K. Yeo for his support and guidance on this project. I also extend additional thanks to Dr. Yeo as our class advisor for the entire Master's program. I am also grateful to Gernot S. Pomrenke and Jose E. Colon for their expertise in this area from which a large portion of my understanding came. To Greg Smith, I give many thanks for all his efforts in keeping the laboratory up and running. I am also thankful to Mr. Evans and Mr. Cannon for their assistance. Additional thank goes to the Avionics Laboratory for the use of their annealing facility. I must also not forget to thank Ian Brown from the University of California for implanting the samples used in this study.

I want to especially thank my wife Martha for giving me that extra care and understanding during this project. I could not ask for any more than she cheerfully gave to make this an enjoyable experience. I am thankful to have had the opportunity to attend AFIT and have greatly benefited from the experience.

Michael B. Scott

List of Figures

List of Figures (cont.)

List of Tables

Abstract

Actinides, like lanthanides, have a partially filled inner shell (5f for actinides) so that semiconductors implanted with these elements should have sharp emissions characteristic of the atomic transitions of the free element ions. In this work, III-V semiconductors GaAs, GaP, and InP and ternary $Al_{0.15}Ga_{0.85}As$ were ion implanted with Uranium 238 using an energy of 350 keV, at a dosage of $4 \times 10^{13}/cm^2$. The samples were proximity annealed using conventional furnace annealing methods from 575 to 950 C with N_2 forming gas for ten minutes. A low temperature photoluminescence study was then done on the samples. All samples were examined at 7 K from the luminescence wavelength of .8 to 1.8 microns. Uranium-associated emissions were observed in the near infrared region in each semiconductor type except for n-type GaP. The uranium emissions in n-type GaP were too weak to confirm. An annealing temperature dependence study and a sample temperature dependence study were done to associate emissions to specific centers and observe thermal quenching. Thermal quenching of uranium emissions varied between samples with the highest sample temperature being 120 K for $Al_{0.15}Ga_{0.85}As$. No effects by the doping of uranium were observed in the band edge emissions except in semi-insulating (SI) InP:U.

The optimum annealing temperature for SI-GaAs, SI-InP, and n-type $Al_{0.15}Ga_{0.85}As$ was 700 C. For n-type GaAs, the optimum an-

nealing temperature was 750C. The increase in emission intensities with higher annealing temperatures suggests a lattice site luminescence center. The similar intensity dependence on sample temperature by each Uranium emission in each semiconductor, implies a single luminescence center. For SI-GaAs, n-type GaAs, and n-type $Al_{0.15}Ga_{0.85}As$, a similar luminescence center exists while the SI-InP appears to form a different luminescence center. The uranium emissions in n-type $Al_{0.15}Ga_{0.85}As$ and n-type GaAs are the same as in SI-GaAs, but less intense, indicating a dependency on host conductivity for the uranium's radiative efficiency. The weakness of uranium emissions shows that uranium-doped semiconductors must be modified to significantly improve the quantum efficiency of the radiation transfer process before they can be seriously considered for use in devices.

LOW TEMPERATURE PHOTOLUMINESCENCE STUDY OF URANIUM IMPLANTED INTO III-V SEMICONDUCTORS AND AlGaAs

Chapter I

Introduction

The need for developing new optoelectronic devices is a concern of the Air Force as we approach the twenty-first century. This is primarily due to the heavy emphasis placed on quality over quantity in maintaining a deterrent force. In recent years, rare earth elements incorporated into semiconductors have shown promise in the development of such devices as light emitting diodes (LEDs) and injection lasers. Their characteristic strong and sharp emissions in the infrared and near infrared regions are advantageous in fiber optic communications as they will allow higher transmission rates over longer distances. For example, silica-based fiber optics have their minimum attenuation at a wavelength of 1.5 microns and semiconductors doped with erbium have strong emissions also at 1.5 microns, making longer transmissions distances possible with less additions of stationed signal amplifiers.(1) In addition to meeting the minimum attenuation requirements, these emissions have narrow bandwidths which minimizes the dispersive effects of fiber optics and thus allow higher transmission rates. However the United States is lagging behind such countries as the Soviet Union, West Germany, Japan, France, and Poland in this area of research. It is therefore of extreme importance that the Air Force establish a serious re-

search effort in this area.

Rare earth 4f-4f emissions in semiconductors correspond to nearly free rare earth ion emissions due to their unique electronic configuration : their outer shells shield the 4f shell from the crystal field of the semiconductor. Actinides also have a partially filled inner shell (5f) and so their 5f-5f emissions will also be very similar to their free ion emissions. It is this comparable situation that makes the investigation of actinides the next logical step. Understanding the mechanism behind 5f transitions will allow future research to proceed in a productive manner in the development of new devices incorporating actinides.

This research was on the actinide uranium (U) implanted into III-V semiconductors and the ternary $Al_{0.15}Ga_{0.85}As$. III-V semiconductors and AlGaAs are widely researched semiconductors, not only by the Air Force, but throughout the optoelectronic industry. Included in this research was an optimization study of annealing temperatures. Conventional annealing was the only method used due to a limited number of samples. The optimum annealing temperature varied between semiconductors. Semi-insulating (SI) GaAs gave the strongest uranium emissions of all the semiconductors when annealed at 700 C. For n-type $Al_{0.15}Ga_{0.85}As$ and SI-InP, the optimum annealing temperature was also 700 C. The weakest signals came from n-type GaAs and n-type GaP. Any signals from the n-type GaP sample were too weak to study. The best annealing temperature for n-type GaAs was 750 C. Available samples

were with different conductivities were only for GaAs, allowing some determination of conductivity effects on uranium emissions. The semiconductors used were semi-insulating (SI) GaAs, n-type GaAs, SI-InP, n-type $Al_{0.15}Ga_{0.85}As$ (15% aluminum and 85% gallium), and n-type GaP.

The goal of this research was to observe the uranium characteristic emissions in the implanted semiconductors by low temperature photoluminescence. Other objectives included determining annealing temperature dependence, substrate dependence, and gaining information on luminescent centers. To date, uranium emissions have been seen in SI-GaAs and InP.(2)

Photoluminescence research sheds only a little light on what mechanisms and structures are occurring in these doped semiconductors. Selective photoluminescence, lifetime measurements, and other research is needed to build a complete picture. Uranium may turn out not to be a candidate for building devices, however, the work done will still be extremely useful as it will add to our understanding of these radiative processes. The main divisions of this document are the background, general theory and previous work in chapter II; experimental set-up and procedures in chapter III; results in chapter IV; and conclusions and suggestions in chapter V.

Chapter II

Theory and Previous Work

A. Introduction to Semiconductors

In a crystal, electrical conductivity due to the free electron motion only arises from the electron motion in the partially filled energy bands. In the simplest quantum mechanical view of an electron in a crystal, the electron is in a perfectly periodic potential. When the Schrodinger equation is solved for this arrangement, allowed electronic energies occur in bands separated by forbidden energy regions.(3:208) A semiconductor acts like an insulator at zero degrees Kelvin because there are no partially filled energy bands. The lower bands are completely full while the upper bands are completely empty. The energy gap between the top of the highest filled band (valence) and the bottom of the lowest empty band (conduction) is known as the bandgap. As the temperature increases, some electrons in the valence band are thermally excited into the conduction band creating vacancies in the valence band. Both the excited electrons and vacancies (known as holes) are free to move through the crystal and are therefore charge carriers. The holes are positive charge carriers while the electrons are, of course, negative charge carriers. It is easy to see that as the temperature increases, the semiconductor behaves more like a conductor and less like an insulator as the number of electrons in the conduction band and holes in the valence band increase.

Figure 1 shows a diagram of the bandgap (forbidden region) separating the conduction and valence band at 0 K and at room temperature.(3:257)

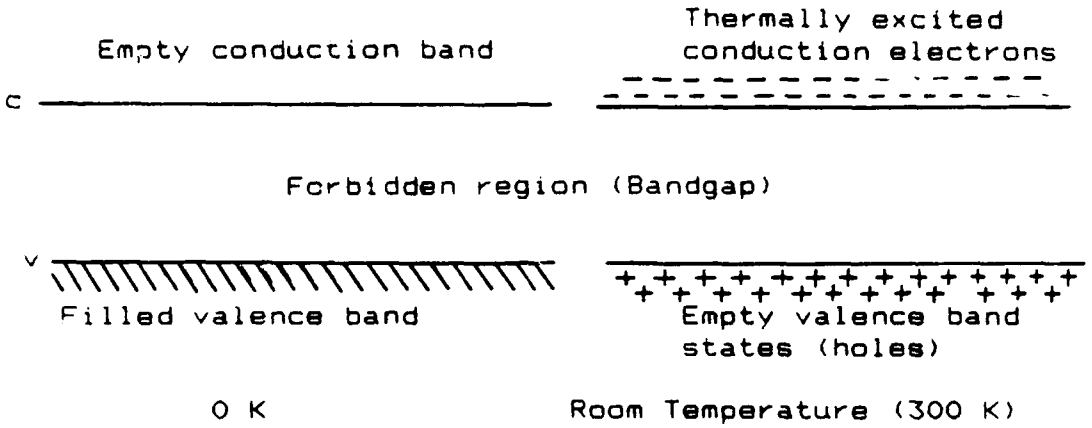

Figure 1. Bandgap (forbidden region) Diagram of a Semiconductor at 0 K and Room Temperature (300 K).

Though called the forbidden region, this bandgap can contain energy levels due to impurities and to the presence of lattice defects in the semiconductor. Even the best produced semiconductors will have some impurities and defects. If particular energy levels in the forbidden region are desired, impurities can be deliberately added. This process is called doping.

An impurity that replaces an atom in the crystal and has more valence electrons than the atom it replaces is known as a donor since it will donate those surplus valence electrons to the conduction band relatively easily. In this situation, the semiconductor is known as n-type. This donor energy level usually lies

just below the conduction band as it usually takes little energy to ionize the donor by exciting these surplus electrons into the conduction band. If the impurity has fewer valence electrons than the atom it replaces, then it will easily accept electrons from the valence band of the crystal and is known as an acceptor. Crystals with this type of impurity are called p-type semiconductors. The acceptor energy level is usually just above the valence band as it also usually takes little energy to ionize the acceptor. The extra electrons (or holes) of the impurity are bound to the impurity atom only by electrostatic forces which are quite weak and can be easily freed through thermal excitation. (3:261) The energy needed to ionize the impurity center is given by: (3:268)

(1) $$E_i = - m^* e^4 / 2n^2 k^2 \hbar^2$$

where:

- e electronic charge
- m^* effective mass of electron or hole
- k relative dielectric constant of crystal
- n integer
- $\hbar$ Planck's constant divided by 2π

Defects will also produce energy levels in the bandgap. One type of defect is a vacant lattice site (vacancy defect) which changes the potential of the crystal at and around the vacant site. Another defect involved an atom which is located not at a lattice site but between sites (interstitial defect). Still another defect occurs when a semiconductor made of two different elements has the opposite element at a lattice site (anti-site

defect). For example, in GaAs an anti-site defect is when a gallium atom is at a arsenic site or vice-versa.

Another energy level in the bandgap may be due to an exciton. The exciton is a quantum of electronic excitation energy traveling in a periodic structure consisting of an electron-hole pair orbiting around its center of mass and is charge neutral thereby transferring only energy (no charge).(4:1) The orbit is due to the Coulombic force (e^2/r). In a crystal this attractive force is reduced by the crystal's dielectric constant (k) resulting in a larger orbit (Figure 2).(4:16)

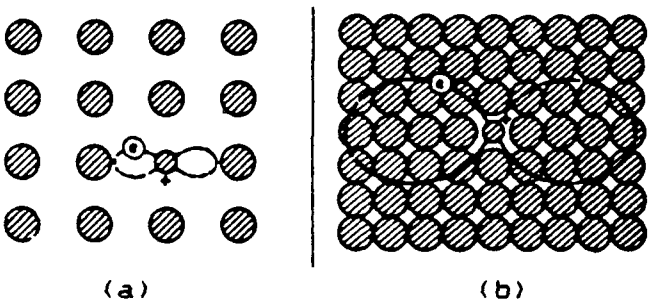

Figure 2. Schematic illustration of the transition from (a) the tight-binding exciton, to (b), the weak-binding exciton.

The energy of an exciton is obtained by solving the Schrodinger wave equation. The energy of the exciton is given by: (5:12)

$$E_{ex} = - m^* e^4 \hbar^2 k^2 n^2 / 2 \qquad (2)$$

where m is the reduced mass obtained by using the effective masses of the electron and hole and n is the quantum number of the exciton state.

Two types of excitons exist - bound and free. Bound excitons are bound to impurity centers in the crystal, whereas free excitons move freely through the crystal. The bound exciton has the lesser energy by an amount dependent on the trapping impurity.

1. Ion Implantation and Annealing

Many methods exist to incorporate dopants into semiconductors. Each method has its advantages and disadvantages. Ion implantation has the advantage of being able to accurately control the concentration of the dopant and thus samples can be readily duplicated. However, it has the disadvantage of severely damaging the crystal lattice, creating vacancies, interstitials and anti-site defects. In ion implantation, a beam of high energy particles are fired into the crystal. The beam is scanned over the sample to evenly implant the ions. The kinetic energy of the ions determines the depth profile of the ions in the crystal. To avoid a phenomenon known as channeling, the beam is placed at a slight angle to the normal of the crystal plane. Channeling is where some ions will travel along interstitial corridors where there is little to slow them down and so the depth profile losses its Gaussian-like shape.

The result of ion implantation is that the ions travel into the crystal disrupting the crystal's order and leaving the ions mostly at interstitial positions. By annealing the implanted samples, the crystalline order can be almost completely restored and most of the ions will position themselves in lattice sites. There are numerous ways to anneal a sample such as rapid thermal annealing (RTA), laser annealing, and conventional furnace an-

nealing. For zincblende crystals, RTA and conventional furnace annealing are the preferred methods. We will be concerned only with conventional furnace annealing as this was the only method employed in this research.

In conventional furnace annealing, the sample is placed into an annealing tube which is then inserted into a preheated oven, and heated at a set temperature for a fixed length of time. Flowing gas is passed through the tube (usually H_2 or N_2) to prevent any contamination to the crystal (see figure 3). At these high temperatures, the ligands (i.e., P in InP) will attempt to diffuse out of the surface and create vacancy defects. To minimize this problem, the sample is either capped with a chemical film (encapsulation) or an unimplanted semiconductor with the same ligand is placed on the sample's surface (proximity method) as shown in figure 3.

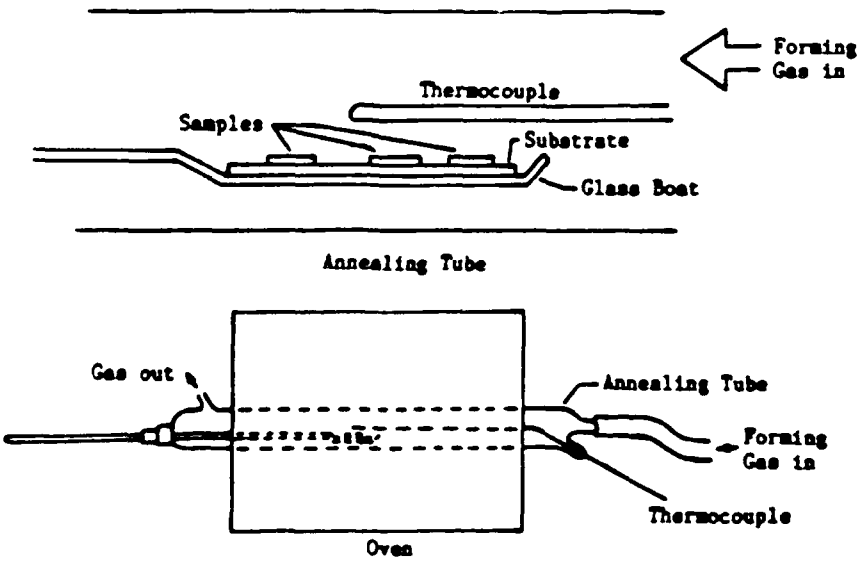

Figure 3. Conventional Annealing Setup

(top - annealing tube, bottom - tube in annealing oven)

Of course, the annealing process is not without undesirable effects. As the crystal is reordering itself, the implanted ions tend to migrate toward the surface and/or into the sample thereby altering the distribution profile. Earlier profile analysis of uranium in GaAs has shown this migration to be minimal in conventional furnace annealing.(2)

2. Photoluminescence, Radiative and Nonradiative Transitions

To gain an understanding of the structure and properties of a semiconductor, photoluminescence can be used. It is a non-destructive technique unlike electroluminescence where ohmic contacts must be soldered to the sample. Information on both the crystal (intrinsic) and the impurities and defects (extrinsic) can be discovered using photoluminescence. Photoluminescence spectroscopy is the process of exciting a sample with light and examining the resulting luminescence spectrum from the sample using a spectrometer-detector setup. The excitation light's frequency must be high enough so that its associated energy ($E = h\nu$) is greater than the bandgap energy of the semiconductor. Lasers are usually employed as the excitation source, although, other sources have served well in the past.(6)

The semiconductor will absorb the light by the excitation of an electron from the valence band to the conduction band. Once excited, the electron will begin a series of relaxation transitions back to the valence band. Some of these transitions will result in photon emission and are known as radiative transitions. The frequency of the emission will be associated with the change in energy levels of the electron ($\Delta E = h\nu$). The other transi-

tions are called nonradiative transitions as they either emit only phonons or they excite other impurities. Figure 4 shows some of the main radiative transitions in semiconductors. The solid and broken lines indicate radiative and nonradiative transitions, respectively. The radiative transitions are what make up the luminescence spectrum and characterizes the intrinsic and extrinsic nature of the semiconductor.

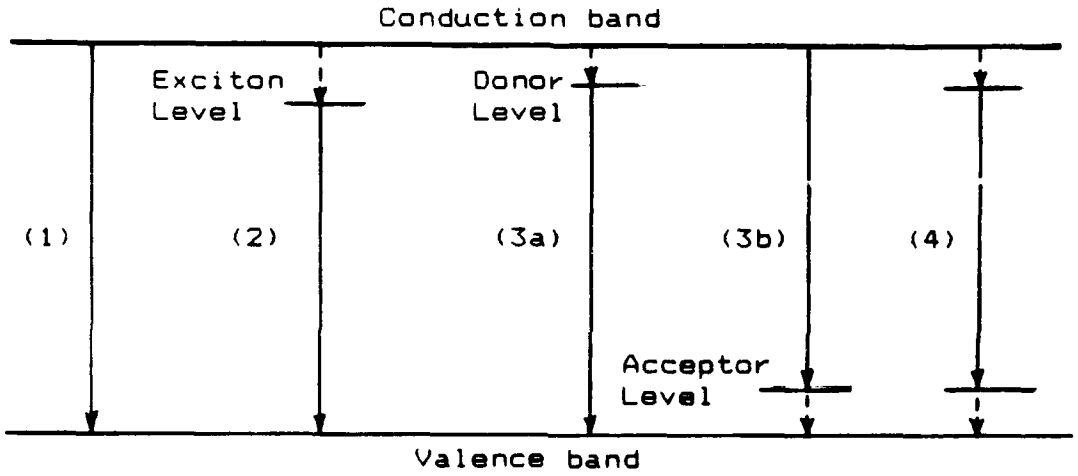

Figure 4. Common Transitions in Semiconductors

(1) band to band recombination

(2) exciton recombination

(3) free to bound transition

(4) donor-acceptor transition

2.a. Band-to-Band Recombination

After an electron has been excited into the conduction band, it will nonradiatively relax to near the bottom of the con-

duction band. In a direct recombination, the electron will then recombine with a hole near at the top of the valence band without the assistance of any intermediate step (transition 1 in figure 4), generating a photon of energy nearly equal to the bandgap energy (E_g). In order to conserve momemtum, the recombining electron and hole must have k-vectors such that $\vec{k}_p + \vec{k}_n = 0$. If the energy minima of the conduction and maxima of the valence bands are not at the same wave vectors the transition will invoive the emission or absorption of phonons (indirect), and the frequency will be slightly shifted by the energy associated with those phonons.

2.b. Excitons

i. Free Excitons

The recombination of the electron and hole of a free exciton causes the emittance of a photon of energy equal to the difference between the bandgap (E_g) and excitonic (E_x) energies. (5:114)

ii. Bound Excitons

When a bound exciton is extinguished by the recombination of the oroiting electron and hole, a photon of energy ($h\nu = E_g - E_x - E_b$) is emitted, where E_b is the additional binding energy which varies according to the binding center.(5:120)

2.c. Free to Bound Transitions

This type of transition occurs when an electron in the conduction band relaxes to an acceptor level or an electron in a donor level relaxes to the valence band (transitions 3a and 3b in figure 4). The energy associated with the emitted photon is

equal to the difference between the bandgap energy (E_g) and the ionization energy of the acceptor (E_a) or donor (E_d). (5:132)

2.d. Donor-Acceptor Pair Transitions

Now that we have donor and acceptor levels in the forbidden region, another possible transition involves the electron relaxing from the donor level to the acceptor level (transition 4 in figure 4). The energy associated with this transition will be equal to the difference between the two energy levels plus an amount equal to the Coulombic attraction between the electron at the donor site and the hole at the acceptor site. (5:143)

(3) $$E_{da} = E_g - E_a - E_d + e^2/kr$$

where: E_a is the acceptor's ionization energy

E_d is the donor's ionization energy

3. Lattice Vibrations and Phonon Replicas

To this point we have considered transitions in a static average field. Now the effect of the dynamic lattice modes, $H_{elec\text{-}dynamic}$, on the radiative transitions must be taken into account. When this term is included in the Hamiltonian of the system, the probability of an optical transition being accompanied by a change in the phonon state becomes nonzero. Thus, the sharp no-phonon emission may be accompanied by sidebands of one-, two-, and so on phonon emissions. These sidebands are known as phonon replicas. (7:12)

4. Line Broadening

For the radiative transition lines, two types of line broadening processes can occur: inhomogeneous and homogeneous. Due to

nonuniformity of the crystal by growth strains, impurities, dislocations, etc., the optically active ions will experience slightly different pertubations. Since the line frequency of a transition is dependent on the ion's environment, a range of transition frequencies results instead of just a single transition frequency. However, for actinide doped semiconductors, the 5f orbital of the actinides are greatly shielded from the crystal field, inhomogeneous broadening should be quite small. Homogeneous broadening is due to the finite lifetime of the initial and final states of a transition. The uncertainty in a state's energy (ΔE) is related to the lifetime (t) by $\Delta E t \geq \hbar$. For decay rates of 10^{11} s^{-1}, ΔE is about 1 cm^{-1}. (7:20)

B. Optical Properties of Actinides and Past Work

The implantation of actinides in semiconductors is a relatively new occurrence in solid state physics. This is due to the difficulty of handling radioactive and artificial actinides; due to the high affinity of actinides for oxygen and other impurities; and due to the fact that actinides are the most complex group on elements to model energy levels. New techniques in handling and implantation have made implantation easier, and better parameterizations of actinides have been introduced, however, no models have been developed that effectively explain the incorporation of actinides into semiconductors. (8:364)

The electronic configuration of the actinides can be written as:

$$[Rn]5f^n6d7s^2 \quad n = 0,2,3,4,7,8,14$$

or $$[Rn]5f^n7s^2 \quad n = 6,7,9,10,11,12,13,14$$

or $$[Rn]6d^27s^2$$

It is this partially filled 5f orbital that gives the actinides their characteristic sharp emission lines. The outer shells tends to shield the 5f electrons from the crystal field of the host. By comparing the luminescence of the uranium implanted semiconductors with those of earlier studies, valence assignments can be inferred about the emission centers.

These sharp lines in the infrared and near infrared regions make actinides candidates for optoelectronic devices. In the 1960's, work was done with uranium in alkaline earth fluorides in the area of maser research. Also, crystals of alkali fluorides, alkali earth fluorides, and lanthanide fluorides doped with uranium have shown emission spectra containing many narrow lines and sharp bands associated with uranium centers. These studies have shown that the emissions are from U^{3+} and U^{4+} centers. The ground state for U^{3+} has been assigned as $^4I_{9/2}$ with a configuration of $5f^3$, and the ground state for U^{4+} has been assigned as $^3H_4$ with a configuration of $5f^2$.(9) Additional work was also done with neptunium, plutonium, americium, curium, and einsteinium in CaF_2.(8:300) Uranium is still however the only actinide which has lased.

The effect of the crystal field on actinides is greater than

on lanthanides (rare earth) because the actinides' f orbitals extend out further. This will reduce the energy gap between the J states. The crystal field parameters are about double those for the lanthanides and therefore the Stark splitting is bigger and the admixing of the J states is greater, thus reducing the effect of selection rules for transitions.

In the work done on U^{3+} and U^{4+} in CaF_2, the optical absorption spectra shows the different emissions from the trivalent and tetravalent centers.(9) It is in the samples containing almost 100% of the ions in the tetravalent state that similar emissions result as in the Group III-V and AlGaAs semiconductors studied here (1.6-1.7 micron range). Further evidence for U^{4+} luminescence centers is due to the highly improbabable $^4I_{3/2}$ to $^4I_{9/2}$ transition of Stark split spin orbit levels for U^{3+} being in the observed range. This would require splittings of approximately 400 cm^{-1}, however, the splitting turns out to be only about 200 cm^{-1}.

The ion-phonon coupling is also expected to be stronger than for the lanthanides. Multiphonon processes which involve the ion-phonon coupling to higher orders should also be more probable for actinide ions. The nonradiative decay probabilities are higher in actinides limiting potential lasing transitions to the lower lying J states which have larger energy separations, generally in the infrared and near infrared. The optical pumping efficiency of actinides may be improved by codoping with sensitizer ions using schemes similar to those employed for the lanthanides. The presence of low-lying 6d states can cause extensive

excited-state absorption, limiting oscillation primarily to the infrared.(8:299) This increased sensitivity to the environment increases the importance of selecting a host for actinides. The media should have low vibrational frequencies. To date, the excitation mechanism of the actinide ions in semiconductors is still not known. Additional work such as selective photoluminescence, Zeeman spectroscopy, and lifetime measurements needs to be done to gain a clearer understanding of the excitation mechanisms and luminescence centers.

Chapter III

Description of Experiment

This chapter explains how the semiconductor samples were prepared (section A) and how the laboratory was set up and operated (section B).

A. Preparation of Sample

Each substrate was grown in the <100> direction. The semi-insulating GaAs and InP crystals had resistivities ranging from 10^7 to 10^8 ohm-cm. The GaP sample used was n-type (sulphur doped) with a carrier concentration of $n = 1.0 \times 10^{17}/cm^3$. After cleaning and etching, the samples were ion implanted with uranium 238 using a mean energy of 131 keV. The implantation used an unconventional technique, employing a new type of high current metal ion source - Metal Vapor Vacuum Arc (MEVVA).(10) Due to the spread of charge states of the ion beam (U^{1+} through U^{4+}), an uncertainty in the projected range R_p and straggling R_p results. A mono-energetic beam assumption of the charge state distribution was used with a weighted mean energy of 131 keV in an implantation modeling program (TRIM) to estimate R_p and R_p.(8) The calculated values for R_p and R_p for U^{238} in GaAs were 32.2 and 11.1 nm; in InP they were 36.6 and 13.8 nm; and in GaP they were 37.5 and 10.5 nm, and in $Al_{0.15}Ga_{0.85}As$ they were 29.9 and 10.0 nm, respectively.(5)

Secondary-ion mass Spectrometry (SIMS) depth profiling was performed on unannealed and 750 C annealed InP:U. The profile

was near-Gaussian and the peaks was shifted slightly into the substrate.(2) However, the depth distribution correlated closely to the TRIM prediction. Low diffusion to the surface was also observed for uranium. A dosage of $4 \times 10^{13}/cm^2$ was used to implant the samples. Table I shows the substrate, dopants, and conductivity of the samples studied. As shown, no p-type semiconductors were analyzed.

Table I

Uranium Implanted Substrates

Substrate	Dopant	Conductivity
InP	Fe	SI
GaAs	Cr	SI
GaAs	Sn	n-type
$Al_{0.15}Ga_{0.85}As$	unintentionally	n-type
GaP	Sn	n-type

The size of the samples ranged from 12 to 24 mm^2. The n-type $Al_{0.15}Ga_{0.85}As$ samples were smaller in size due to a limited supply of that particular semiconductor. The samples were cleaned after implantation with trichloroethylene, acetone, methanol, deionized water, and then blow dried using dry nitrogen gas.

All the sample types (both implanted and unimplanted) were proximity annealed at various temperatures, ranging from 500 C to 950 C, using conventional furnace techniques for 10 minutes in a N_2 forming gas. One sample type, SI-GaAs, was annealed at 750 C for 5, 10, 15, and 20 minutes to observe the effect of annealing time duration. Table II shows the anneal temperatures and times

for each sample studied.

Table II Anneal Temperatures and Times

Sample	Anneal Temperature (C)	Anneal Time (minutes)
SI GaAs (sub.)	700	10
SI GaAs:U	575	10
	650	"
	700	"
	740	"
	750	"
	800	"
	850	"
	900	"
	950	"
	750	5
	750	15
	750	20
n-type GaAs (sub.)	750	10
n-type GaAs:U	575	10
	650	"
	700	"
	750	"
	800	"
	850	"
$Al_{0.15}Ga_{0.85}As$ (sub.)	700	10
$Al_{0.15}Ga_{0.85}As$:U	575	10
	650	"
	700	"
	750	"
	800	"
GaP (sub.)	750	10
GaP:U	600	10
	650	"
	700	"
	750	"
InP (sub.)	700	10
InP:U	500	10
	575	"
	650	"
	700	"
	750	"

B. Experimental Setup

The laboratory setup for the photoluminescence study can be broken down into four systems: 1) cryogenic system; 2) excitation system; 3) detection system; and 4) data acquisition system. Figures 5 and 6 show the experimental setup.

1. Cryogenic system

In photoluminescence studies, the sample is usually cooled to very low temperatures to significantly reduce thermal effects and insure that the ground state is the most populated state. This was accomplished using a cryogenic system consisting of a Janis dewar, vacuum system, and DRC 82C temperature controller.

The dewar contains an inner sample chamber, where the sample was cooled by a controlled flow of liquid helium; an intermediate helium reservoir; and an outer nitrogen reservoir. Each section is thermally isolated by high vacuum walls. The nitrogen reservoir and high vacuum around the helium chamber prevent rapid evaporation of the helium. The flow of helium is controlled by a needle valve in the bottom of the helium chamber.

The high vacuum is obtained by first running a mechanical oil pump that would pull to a 50 micron vacuum. To go from 50 microns to 0.1 microns, a turbomolecular pump is then engaged to run in line with the mechanical pump. Once the high vacuum is obtained, the vacuum chamber is sealed and the pumps turned off.

The temperature controller uses wires attached to the sample holder to hold the sample at a programmed temperature. The sample temperature can be set from liquid helium to room temperature.

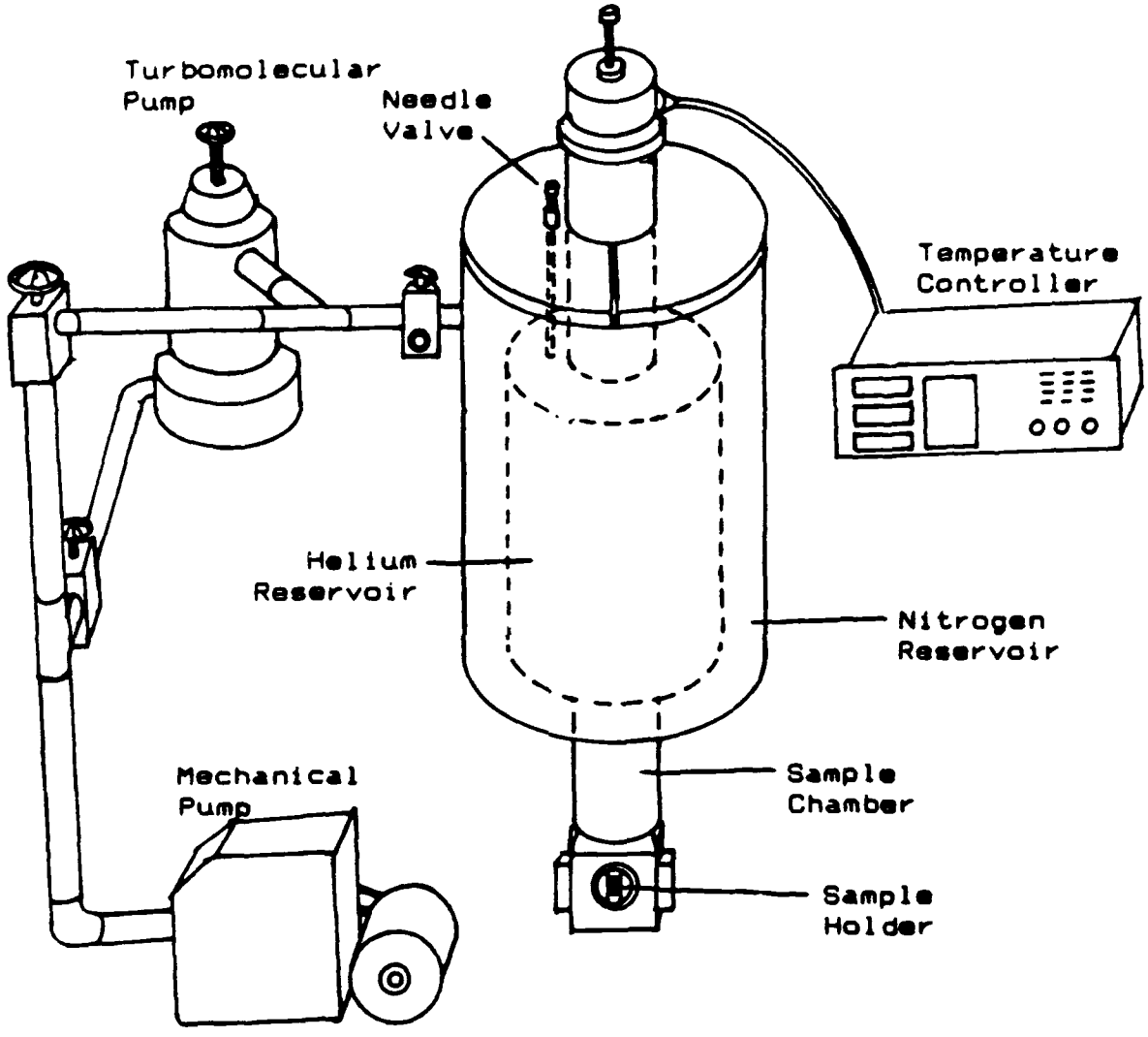

Figure 5. Cyrogenic System - Janis dewar, vacuum system, and temperature controller.

2. Excitation Source

The laser sources used for sample excitation were a water-cooled Spectra Physics 2000 Krypton ion laser at 647.1 nm and an air-cooled ILT 5490 AWC Ar-ion laser at 514.5 nm.

The krypton laser was used at 80, 100, and 200 mW power settings while the Ar-ion laser was used only at 80 mW. The krypton laser was used on every sample. The Ar-ion laser was also used on the n-type GaP samples to provide a laser frequency with an associated energy larger than the GaP band gap energy. The purity of the laser beam was maintained through the use of an interference filter and a short pass near infrared filter. The filtered laser beam was focused onto the sample with irradiances of 2.5, 3.2, and 6.4 W/cm^2.

3. Detection System

To detect and measure the luminescence from the samples, the following equipment was used:

3/4 Meter Czerny-Turner Spectrometer

Nitrogen Cooled Germanium Detector

60 Hertz Chopper

Autoloc Amplifier

Analog-to-Digital Converter

Set of Near Infrared Long Pass Filters

Two focusing lenses

Two voltmeters

Figure 6 shows the setup of this equipment. The spectrometer used a 600 lines/mm grating with a 1.6 micron blaze wavelength.

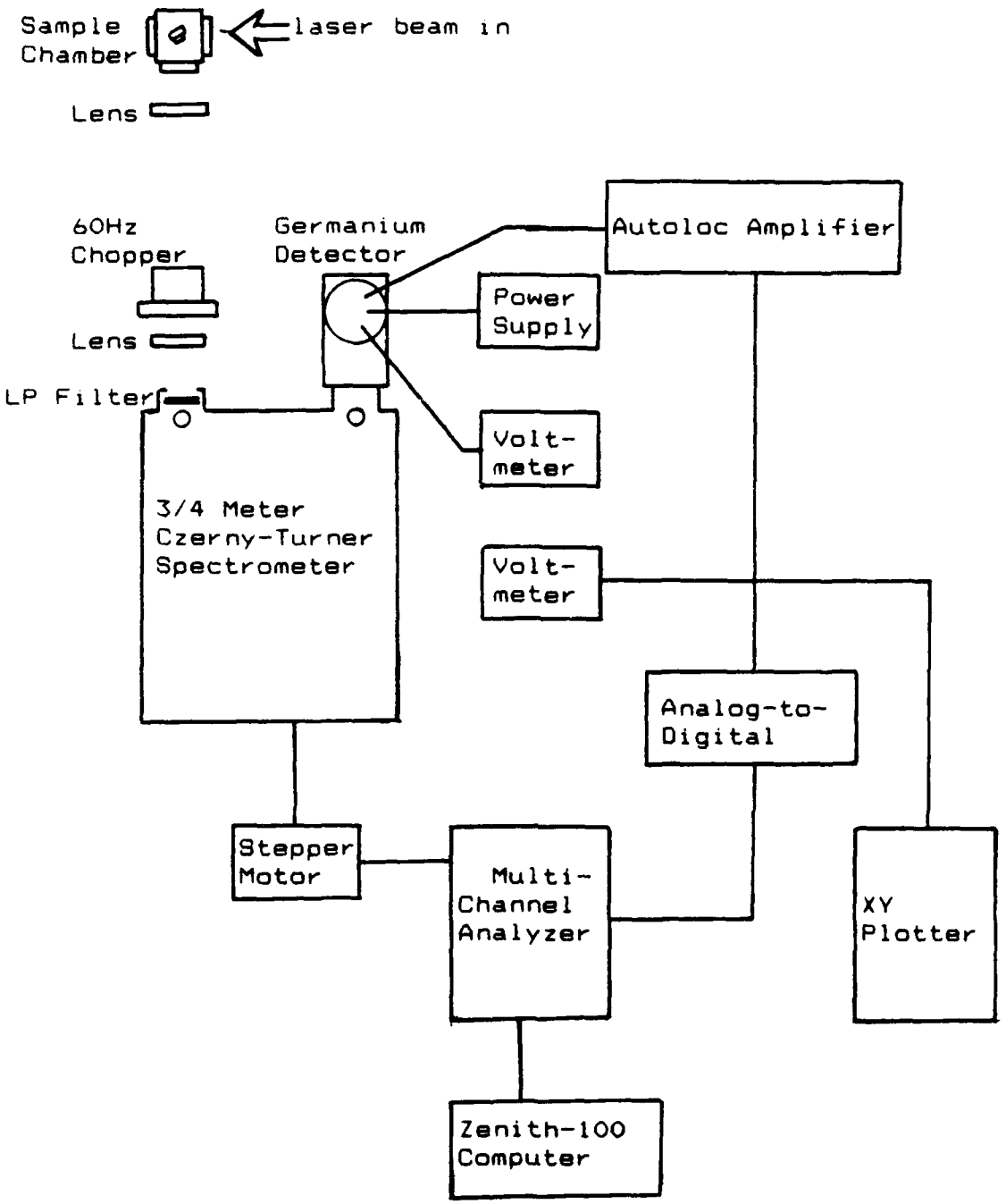

Figure 6. Data Acquisition and Detection System

Due to the relatively weak uranium signals from the samples, most of the spectra were obtained using one and two millimeter entrance and exit slits, respectively.

The germanium detector's spectral response was not factored into the data taken as data was taken over a small range where the response of the detector was fairly constant. The detector was run at a bias voltage of 200 volts. An optional muon filter was available to filter spurious spikes, however, spikes were not found to be a problem and the filter was not used. The detector was kept at a temperature of 77 K by keeping its reservoir filled with liquid nitrogen.

The signal from the detector was fed to the autoloc amplifier where it was amplified and phase locked with the chopper that was placed in front of the entrance slit. From the autoloc amplifier, the signal was sent to the analog-to- digital converter to convert the DC signal to digital form.

Long pass filters were used at the entrance slit of the spectrometer to prevent shorter wavelength signals from entering the spectrometer. This would stop any higher order diffractions from showing up in the spectrum. Two focusing lenses were used between the sample and entrance slit to maximize the collection of luminescence by collimating it and then focusing the image of the sample onto the entrance slit. Efforts were made to find lenses that would match the f-number of the spectrometer, however, this was unsuccessful and some overfilling of the grating resulted. Once a uranium signal was found, the lenses and sample position were adjusted to optimize the signal by monitoring the output of

the detector on a voltmeter connected in parallel with the analog-to-digital converter for this purpose. An additional voltmeter was employed to monitor the detector's voltage to ensure it remained within the specifications.

4. Data Acquisition System

From the analog-to-digital converter, the signal was sent to a Canberra 8100/E Multichannel Analyzer. Additionally the direct analog signal from the autoloc amplifier could be sent to a Hewlett-Packard XY plotter. The multichannel analyzer (MCA) and the 3/4 meter Czerny-Turner spectrometer were synchronized with the use of an adjustable stepper motor. This allowed the flexibility in setting the scanning range from a few angstroms to thousands of angstroms. Once the data was recorded in the MCA, it could be transferred to a Zenith-100 computer and stored onto a floppy disk. Calibration of the spectra was accomplished with the use of a krypton calibration lamp.

Chapter IV

Results and Analysis

The results of the experiment are presented and analyzed in this chapter. It has five sections - one for each emitting semiconductor and a comparison section. Table III summarizes some of the results: giving the annealing temperature, time, and whether an U related signal was detected from each sample studied.

Table III Uranium Emitting Samples

Sample	Anneal Temp. (C) & Time (min)	Uranium Related Emission Seen
SI GaAs:U	575/10	no
	650/10	yes
	700/10	yes
	740/10	yes
	750/10	yes
	800/10	no
	850/10	no
	900/10	no
	950/10	no
	750/5	yes
	750/15	yes
	750/20	yes
n-type GaAs:U	575/10	no
	650/10	no
	700/10	no
	750/10	yes
	800/10	no
	850/10	no
$Al_{0.15}Ga_{0.85}As$:U	575/10	no
	650/10	yes
	700/10	yes
	750/10	yes
	800/10	no
GaP:U	600/10	no
	650/10	no
	700/10	no
	750/10	no
InP:U	500/10	no
	575/10	no
	650/10	yes
	700/10	yes
	750/10	no

A. InP

Figure 7 shows the spectrum of SI-InP:U in the 1.6 micron range at a sample temperature of 7 K for various annealing temperatures (500^{o}C to 750^{o}C). Figure 8 shows the results of SI-InP:U sample annealed at 700^{o}C/10 minute at various sample temperatures. The various spectra are offset along the Y-axis and only signal intensity comparisons can be made from these figures. The zero levels ("no signal" levels) for the spectra are not shown. One and two millimeter slits were used (entrance and exit, respectively) for all spectra in these figures.

Both the sharp peak and the much less intense band (to the left) are uranium related. Both emissions are due to 5f transitions from an excited state to the spin-orbit ground state of the implanted uranium ion (U^{4+} or U^{3+}). The sharp peak corresponds to an energy of 0.743 eV with a full-width at half-maximum (FWHM) of 2.2 meV. Using smaller slits (.1mm & .2mm) the FWHM of the sharp peak was measured as 0.5 meV (not shown). Both the sharp peak and broad band appeared thermally quenched at the same rate as the sample temperature was raised to 110K. This suggests that both emissions are from the same center. In addition, from the increase in signal with higher annealing temperature, the center is probably located at a lattice site. Reduction in signal at the highest temperatures may be attributed to thermal degradation of the semiconductor or to the formation of non-radiative complexes of uranium and impurities.

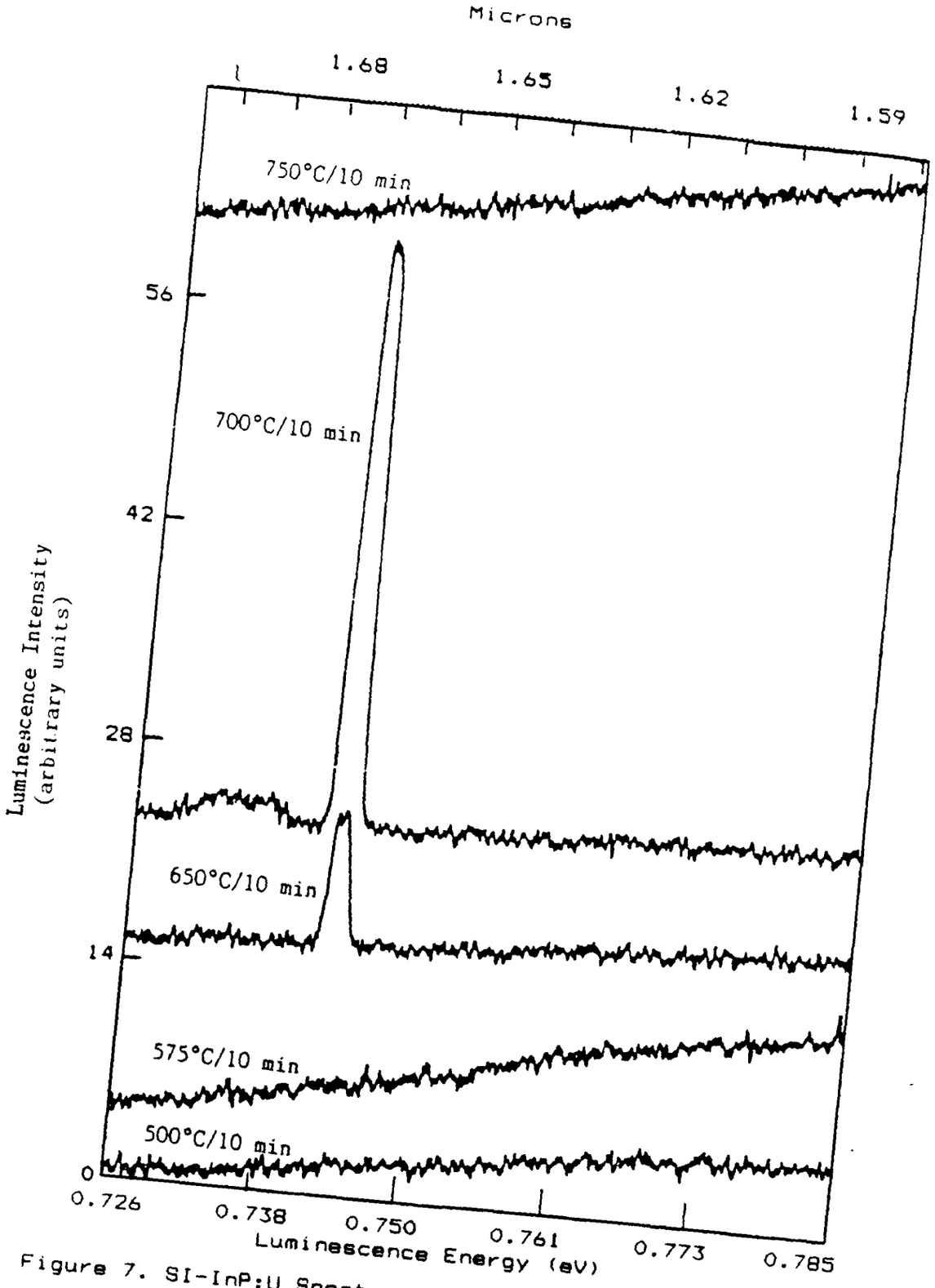

Figure 7. SI-InP:U Spectra at Various Anneal Temperatures

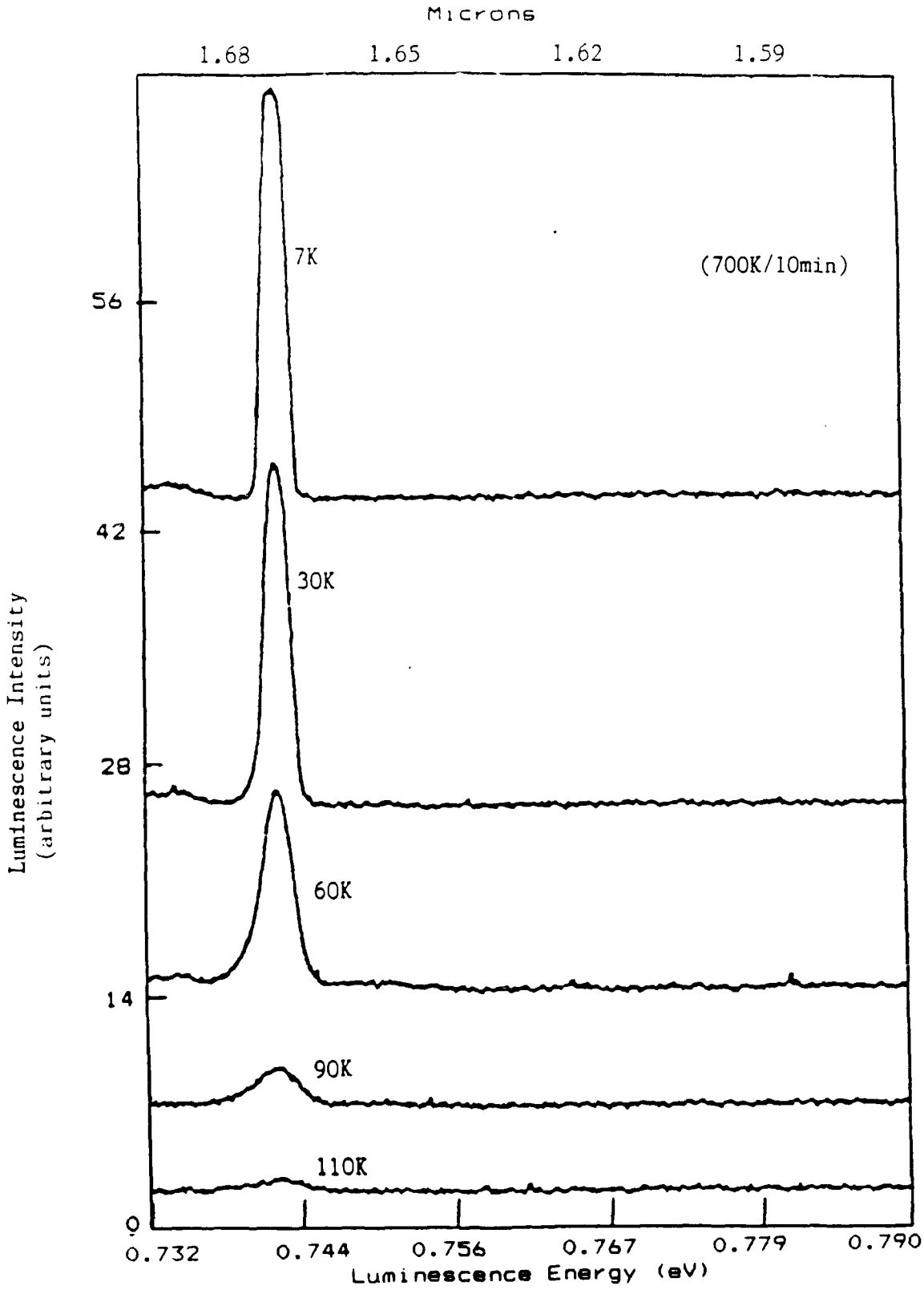

Figure 8. Thermal Quenching of SI-InP:U Spectra for the 700°C/10 min Annealed Sample

The optimum anneal temperature for conventional annealing of SI-InP:U was found to be 700°C. This is for samples annealed conventionally for 10 minutes using the proximity method. Each sample was examined under the same conditions (laser power - 100mW , sample temperature - 7K, slit sizes - 1 and 2 mm, etc.). As can be seen in figure 7, the U signal is quite sensitive to annealing conditions. An earlier sample (not shown) annealed at 750°C for 15 minutes did show the 1.67 micron emission, whereas this 750°C/10 min sample did not. In figure 8, the 1.67 uranium signal starts to rapidly quench after 60K but is still discernible at 110K. Some thermal line broadening can also be seen in the emission.

SI-InP was the only semiconductor tested that had its free-to-bound and donor-acceptor levels quenched by the introduction of uranium. An additional broad band at 1.1 eV was also observed. This band has also been seen in rare earth implanted InP and seems to be related to implantation damage by the heavy ions. This is the first time that the accompanying band at 1.69 microns has been seen. The possibility of this being a phonon replica of the 1.67 line can be ruled out as the transverse optical phonon should have an energy of around 30 meV where as the difference in energy is only around 10 meV. Also the band is too broad to be a phonon replica of the 1.67 line. This band is most likely made up of a few 5f transitions that have much lower transition probabilities. Resolving this band was not possible due to the weakness of the signal and sensitivity limit of the equipment.

No other uranium emissions, either sharp or broad, were

detected between 0.8 and 1.8 microns (the range of the germanium detector). Also, no frequency shift was observed in either signal when the sample temperature was raised.

B. GaP:U

The n-type GaP:U sample did not show any clear uranium emissions. The sample was examined using 1 and 2 mm entrance and exit slits, respectively with a 647.1 nm laser excitation at 100 and 200 mW. The sample was also examined with a 514.5 nm laser line at 80 mW. Neither method resulted in uranium emissions that could be distinguished from the background noise level of the detection system. Various samples of n-type GaP:U were studied. Anneal temperatures ranged from 600 to 750°C. In the region of the observed uranium emissions from other semiconductors, 1.59 to 1.69 microns, only broad non-uranium signals were observed in n-type GaP:U. This may explain why no uranium signals could be detected. Improved GaP:U samples with lower carrier concentrations may give discernible uranium signals.

C. GaAs:U

Two types of GaAs:U samples were examined : semi-insulating (SI) and n-type.

1. SI-GaAs:U

Figure 9 shows the spectra of SI-GaAs:U in the 1.6 micron range at a sample temperature of 7 K for various annealing temperatures (575 to 800°C). Figure 10 shows the results of SI-GaAs:U sample annealed at 700°C/10 minute at various sample tem-

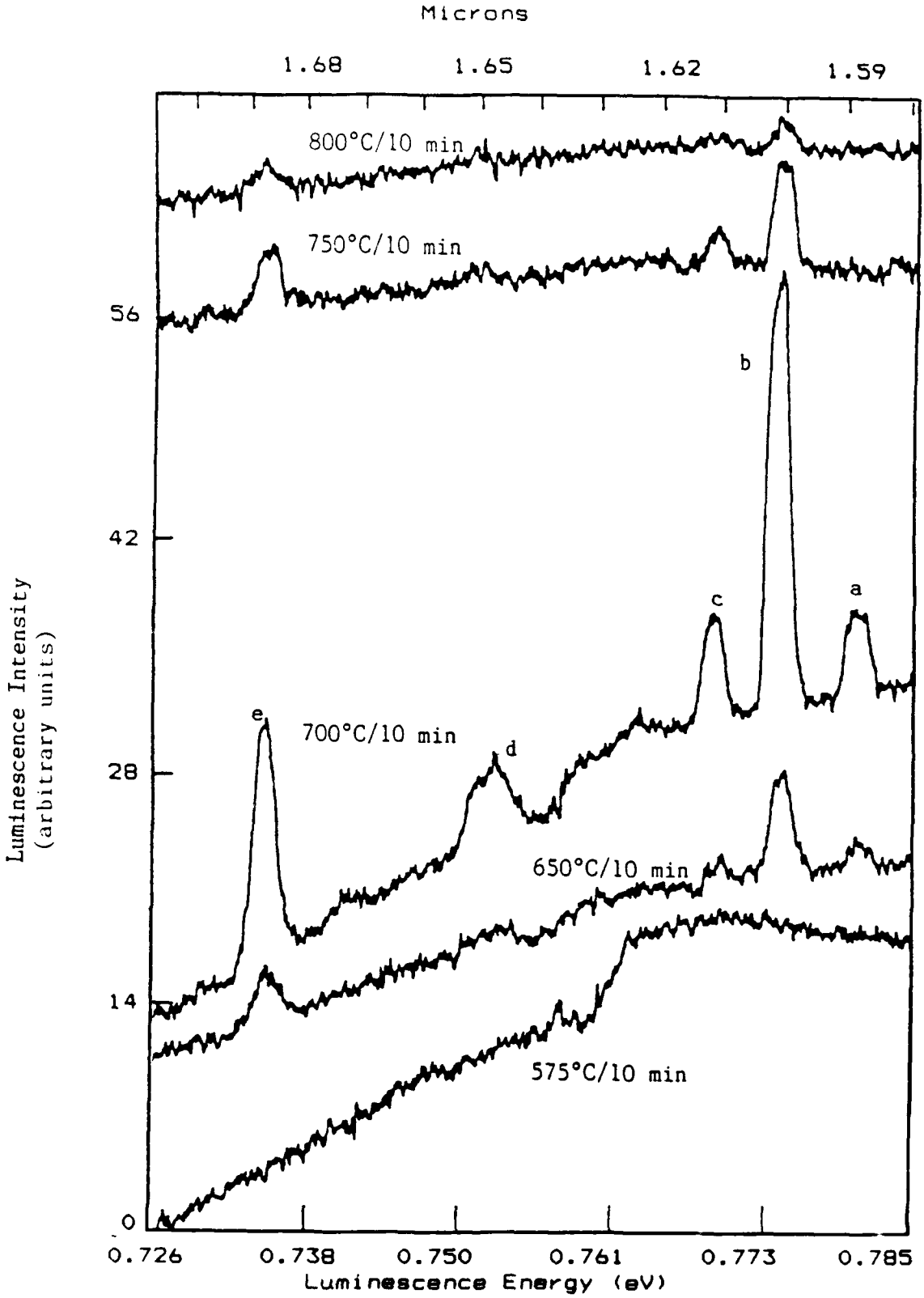

Figure 9. SI-GaAs:U Sample Spectra at Various Annealing Temperatures

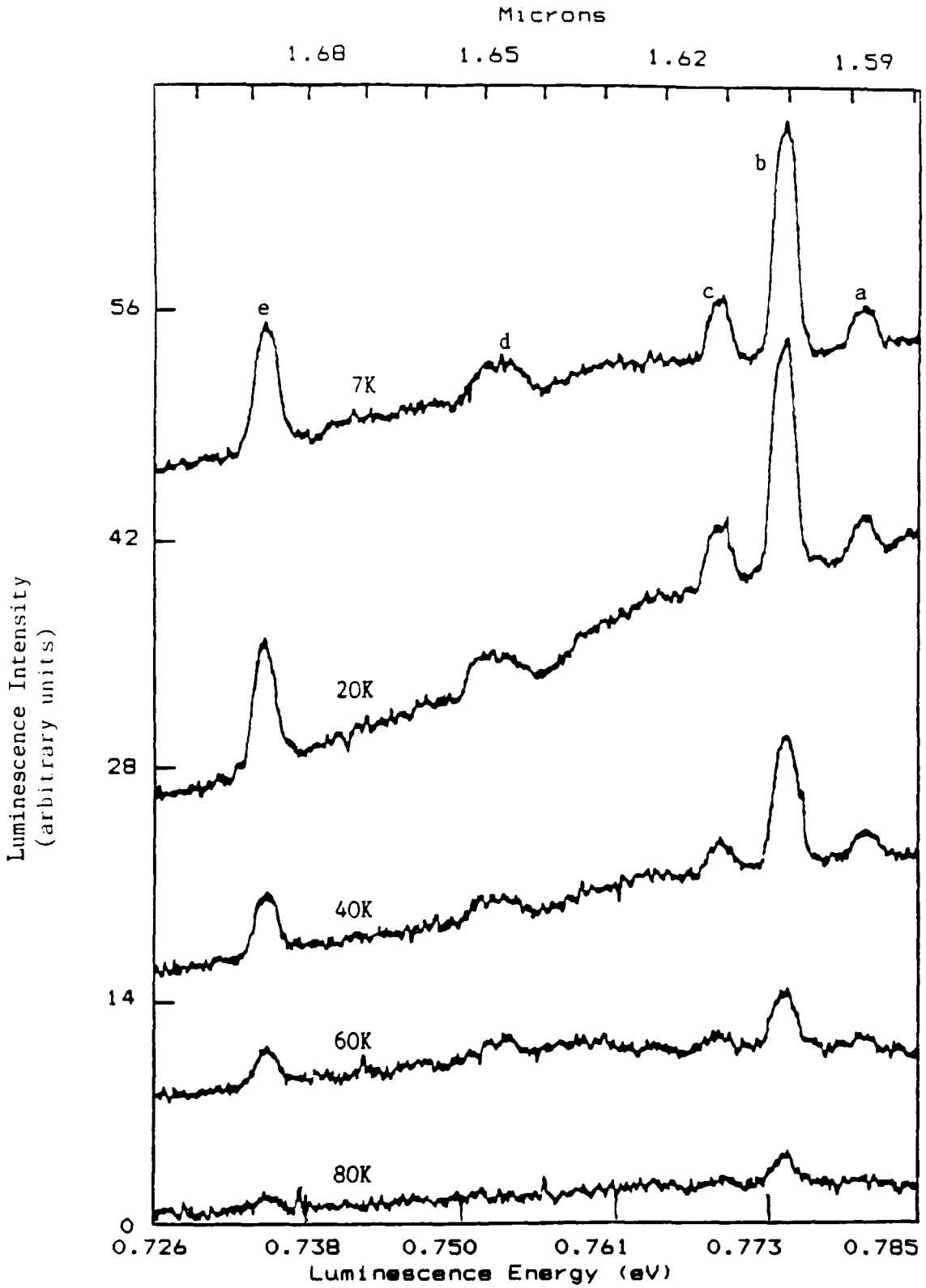

Figure 10. Thermal Quenching of SI-GaAs:U Spectra for the 700°C/10 min Annealed Sample

peratures. Just like the InP:U figures, the different spectra are offset along the Y-axis so that only signal intensity comparisons are possible from these figures. Also, no zero levels ("no signal" levels) can be determined from the spectra. These levels are shown later figure 19. One and two millimeter slits were used (entrance and exit, respectively) for all spectra in these two figures. Each sample was examined under identical conditions (laser power - 100mW , sample temperature - 7K, slit sizes - 1 and 2 mm, etc.).

The five sharp peaks are due to 5f uranium transitions. The emissions represent transitions from excited states to the spin-orbit ground state of the implanted uranium ion (U^{4+} or U^{3+}). Two additional weak emissions may also exist at 1.625 and 1.630 microns. These lines are only revealed in the 700°C/10 min spectrum. The sharpest peak (1.60 microns) corresponds to an energy of 0.773 eV with a FWHM of 2.2 meV. Higher resolution spectra gives a FWHM of 0.5 meV. Figure 11 shows the integrated intensities of the five strongest lines at the various anneal temperatures.

Thermal quenching of all the sharp peaks were equal (reducing to half their 7K intensity by 40K) as the sample temperature was increased through 100K (figure 12). This suggests that all the emissions are from the same luminescence center. The uranium signals start to rapidly quench after 40K. The highest temperature at which the strongest uranium line can be detected is 80K.

From the increase in signal with higher anneal temperatures (up to 700°C), the center can be considered located at a lattice

site. The diminishing intensities at the higher anneal temperatures are probably due to the development of non-radiative complexes formed from uranium ions and impurities. Additionally, above 850°C the anneal temperature can cause crystal structure damage further reducing the uranium signals. For the SI-GaAs:U, the best conventional annealing temperature using the proximity

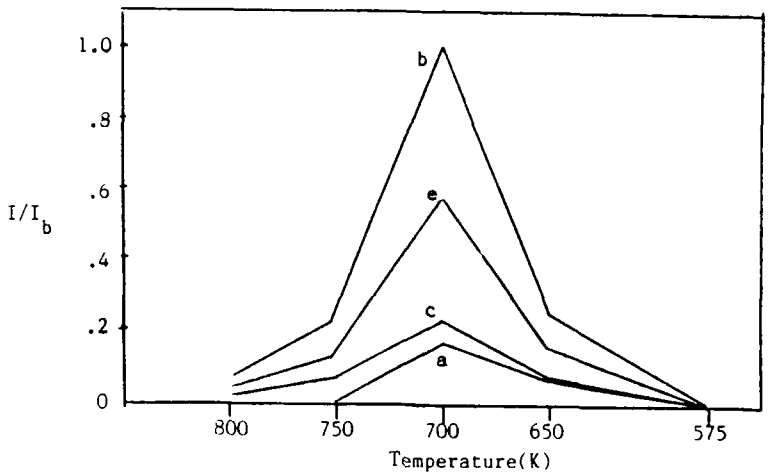

Figure 11. Integrated Intensities of Strongest Uranium Lines at Various Anneal Temperatures (SI-GaAs:U)

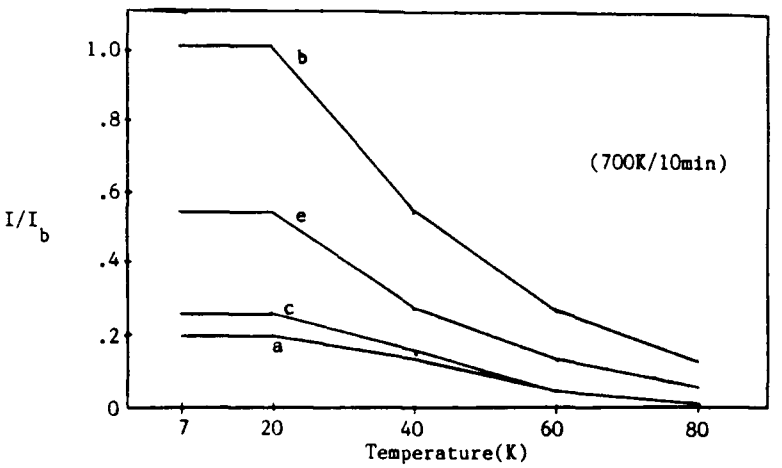

Figure 12. Integrated Intensities of Strongest Uranium Lines for the 700°C/10 min Annealed SI-GaAs:U Sample at Various Sample Temperatures

technique was 700°C.

Three additional SI-GaAs:U samples were annealed at 750°C for 5, 15, and 20 minutes to observe the effect of anneal times on emission intensities (figure 13). The 5 minute annealed sample gave the strongest uranium intensities for all lines. It was the only sample of the four to show the 1.588 micron line. The intensities were reduced approximately by half for all lines when the anneal time was increased to 10 minutes. All the lines were further reduced in half when the anneal time was raised to 15 minutes. For longer anneal times, the reduction in emission intensities appears to slow as the 20 minute annealed sample had approximately the same intensities as the 15 minute annealed sample. The formation of nonradiative complexes could explain this sensitivity to anneal times.

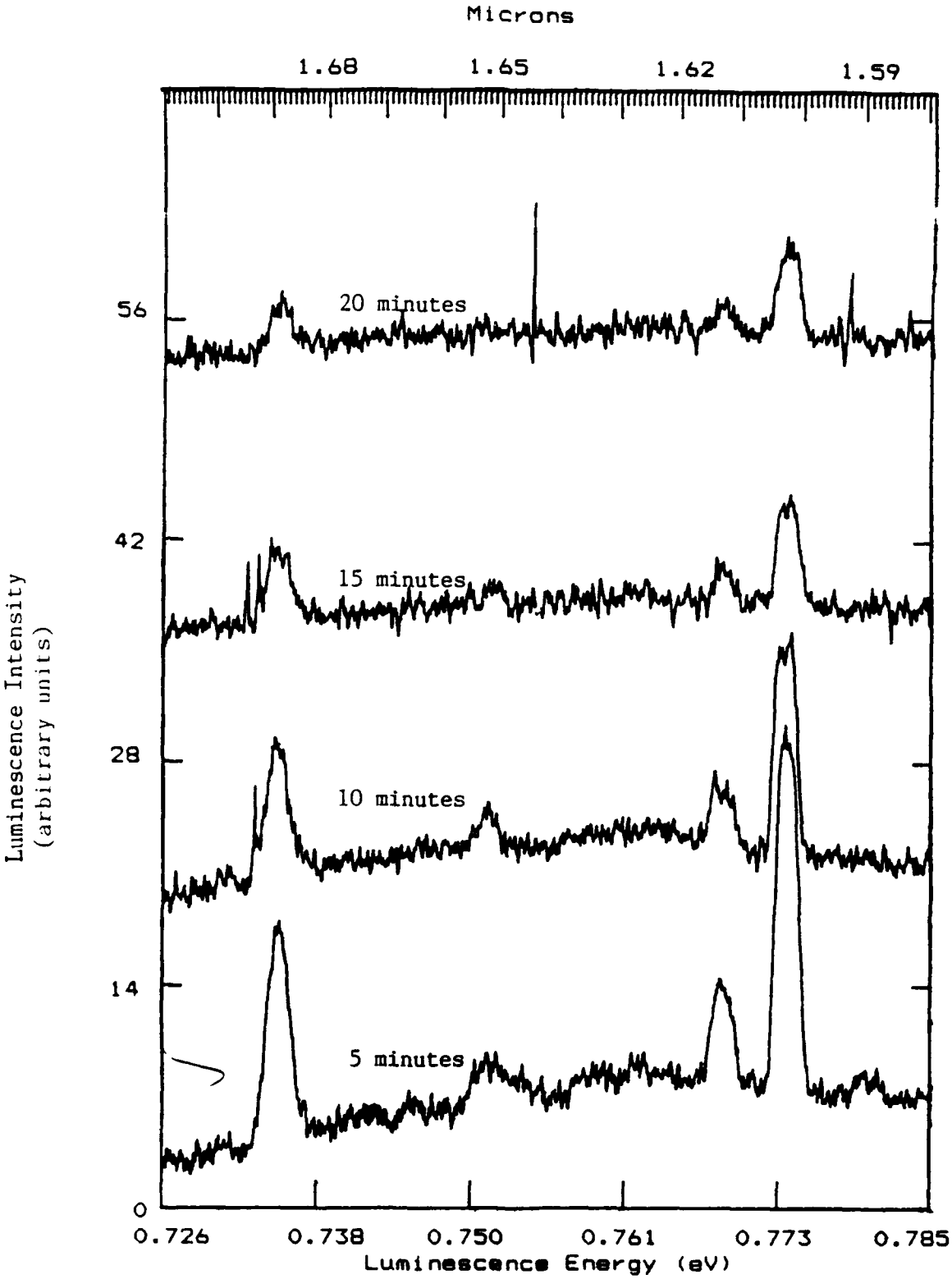

Figure 13. SI-GaAs:U Spectra at Various Anneal Times with a 750°C Anneal Temperature

As can be seen in figures 9 and 11, the U signal intensities are quite sensitive to anneal temperatures. A fifty degree change in anneal temperature from the optimum 700°C anneal temperature greatly reduced the uranium signals. From figure 10, one can see that no thermal line broadening occurs with sample temperature increases. Unlike the SI-InP:U samples, SI-GaAs:U did not have reduced free-to-bound and donor-acceptor levels when compared to an annealed non-implanted sample. The broad band that resides in this range (1.58 to 1.70 microns) is non-uranium related. An earlier study of the semiconductor doped with uranium did not show the 1.59 line.(2) This raises the question as to the association of this line with the other uranium related lines, as the 1.59 micron line is of equal intensity as the 1.63 line in each of the other annealed samples. No other uranium emissions, neither sharp nor broad, were detected between 0.8 and 1.8 microns (the range of the germanium detector). Also, there were no frequency shifts in any of the uranium lines when the sample annealed at 700°C/10 was studied at different sample temperatures.

2. n-type GaAs:U

Figure 14 shows the spectrum of n-type GaAs:U in the 1.6 micron range at a sample temperature of 7K for the 750 and 800°C annealed samples. Figure 15 shows the 1.688 micron line obtained from the n-type GaAs:U annealed at 750°C and measured at various sample temperatures. These figures have their spectra offset along the Y-axis so that only signal intensity comparisons are possible. Likewise, zero levels ("no signal" levels) are not

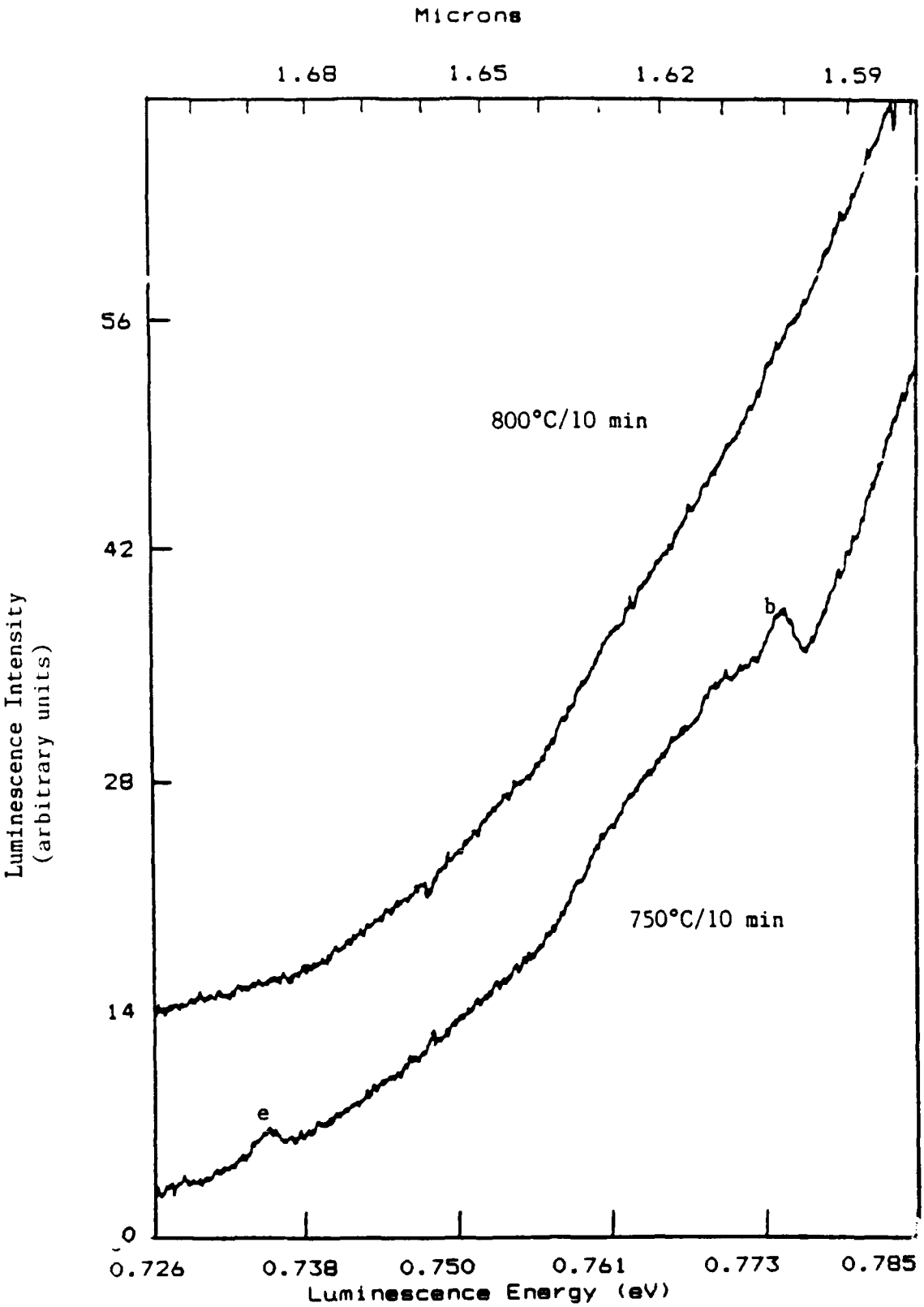

Figure 14. n-type GaAs:U Spectra at Two Annealing Temperatures

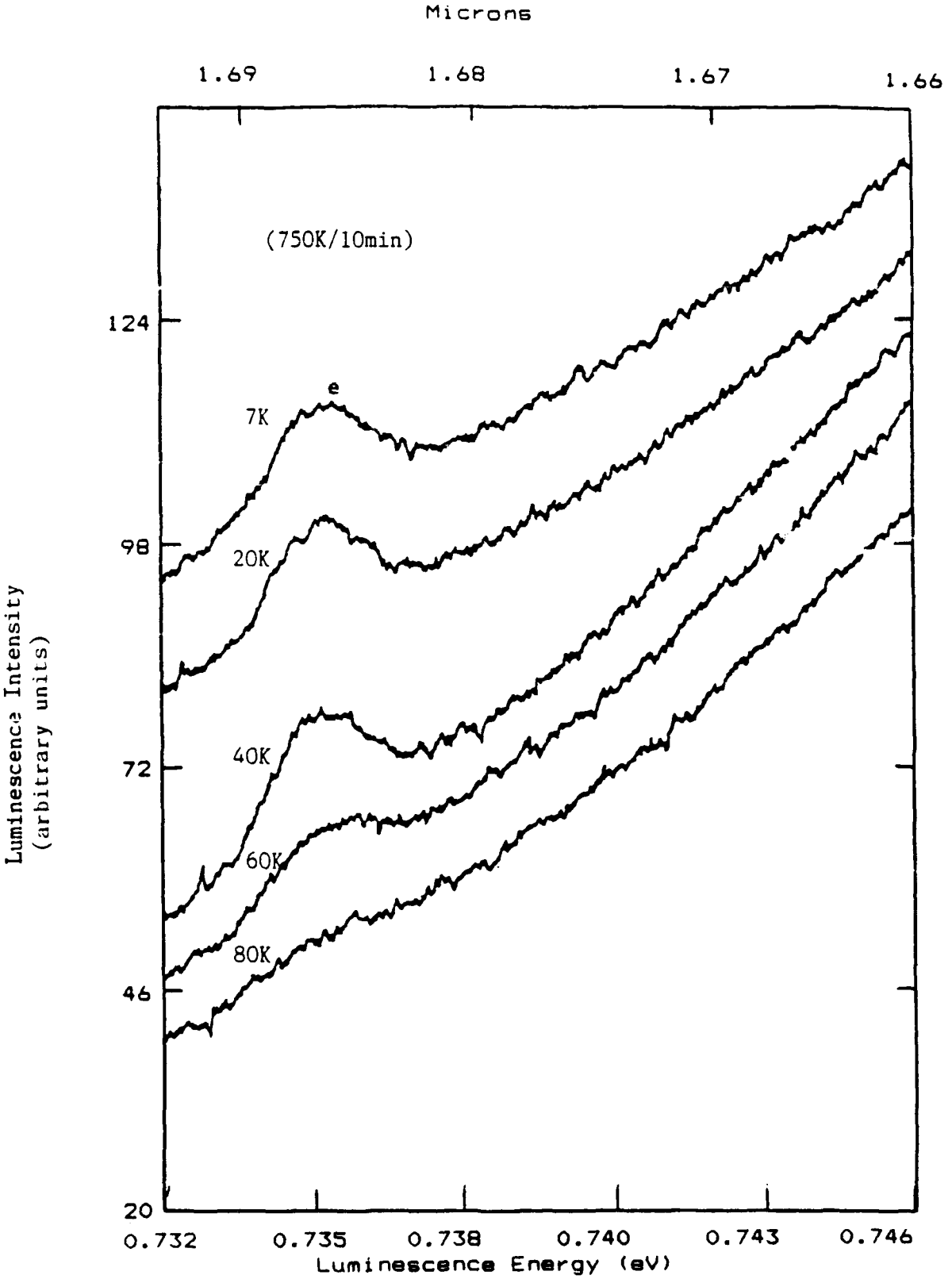

Figure 15. Thermal Quenching of n-type GaAs:U 1.688 line for the 750°C 10 min Annealed Sample

shown for the spectra. One and two millimeter slits were used (entrance and exit, respectively) for the spectra in both figures. Each sample was examined under identical conditions (laser power - 100mW, sample temperature - 7K, slit sizes - 1 and 2 mm, etc.).

The two peaks at 1.688 and 1.60 microns are due to 5f uranium transitions. The emissions are from transitions from excited states to the spin-orbit ground state of the implanted uranium ion (U^{4+} or U^{3+}). The sharpest peak (1.60 microns) corresponds to an energy of 0.773 eV with a FWHM of 2.8 meV. A higher resolution spectra was not possible due to the weakness of emission and sensitivity limit of the detector. Thermal quenching of the two peaks were equal and for better illustration only the 1.688 line is shown in figure 15. The line was discernible through 60K where the thermal quenching increased rapidly. This common thermal quenching behavior between the two peaks suggests a common luminescence center. The samples annealed at temperatures below 750°C had no measurable uranium emissions and are not shown. Because of this, the center can be considered as residing at a lattice site. The loss of the two signals at higher annealing temperatures is probably due to the formation of nonradiative uranium-impurities complexes. The free-to-bound and donor-acceptor levels were not affected by the implanted uranium into the n-type GaAs. A non-uranium related broad band exists in 1.58 to 1.70 micron range which give the spectra their severe slopes. No other uranium emissions, either sharp or broad, were detected between 0.8 and 1.8 microns (range of the germanium detector).

Also, no frequency shift was observed in either signal from sample annealed at 750°C/10 min and measured at different sample temperatures.

D. AlGaAs:U

This is the first time that uranium related emission have been observed in the ternary semiconductor AlGaAs. Figure 16 shows the spectrum of n-type $Al_{0.15}Ga_{0.85}As$:U in the 1.6 micron range at a sample temperature of 7K for various annealing temperatures (575°C to 800°C). Figure 17 shows the results of the n-type $Al_{0.15}Ga_{0.85}As$:U sample annealed at 700°C/10 min and measured at various sample temperatures. Once again, offsets (along Y-axis) were used to display the spectra and only signal intensities can be compared between spectra. Additionally, the zero levels for the spectra are not shown. One and two millimeter slits were used (entrance and exit, respectively) for all the spectra in both figures. Each sample was examined under identical conditions (laser power - 100mW, sample temperature - 7K, slit sizes - 1 and 2 mm, etc.).

Each sharp peak is from a 5f uranium transition. The five emissions are transitions from excited states to the spin-orbit ground state of the implanted uranium ion (U^{4+} or U^{3+}). Another emission may also exist at 1.625 microns. This is only visible in the 700°C/10 min spectrum. The sharpest peak located at 1.60 microns has a FWHM value of 2.8 meV. Using smaller slits (0.4 and 0.8 mm), a higher resolution FWHM of 0.6 meV was measured.

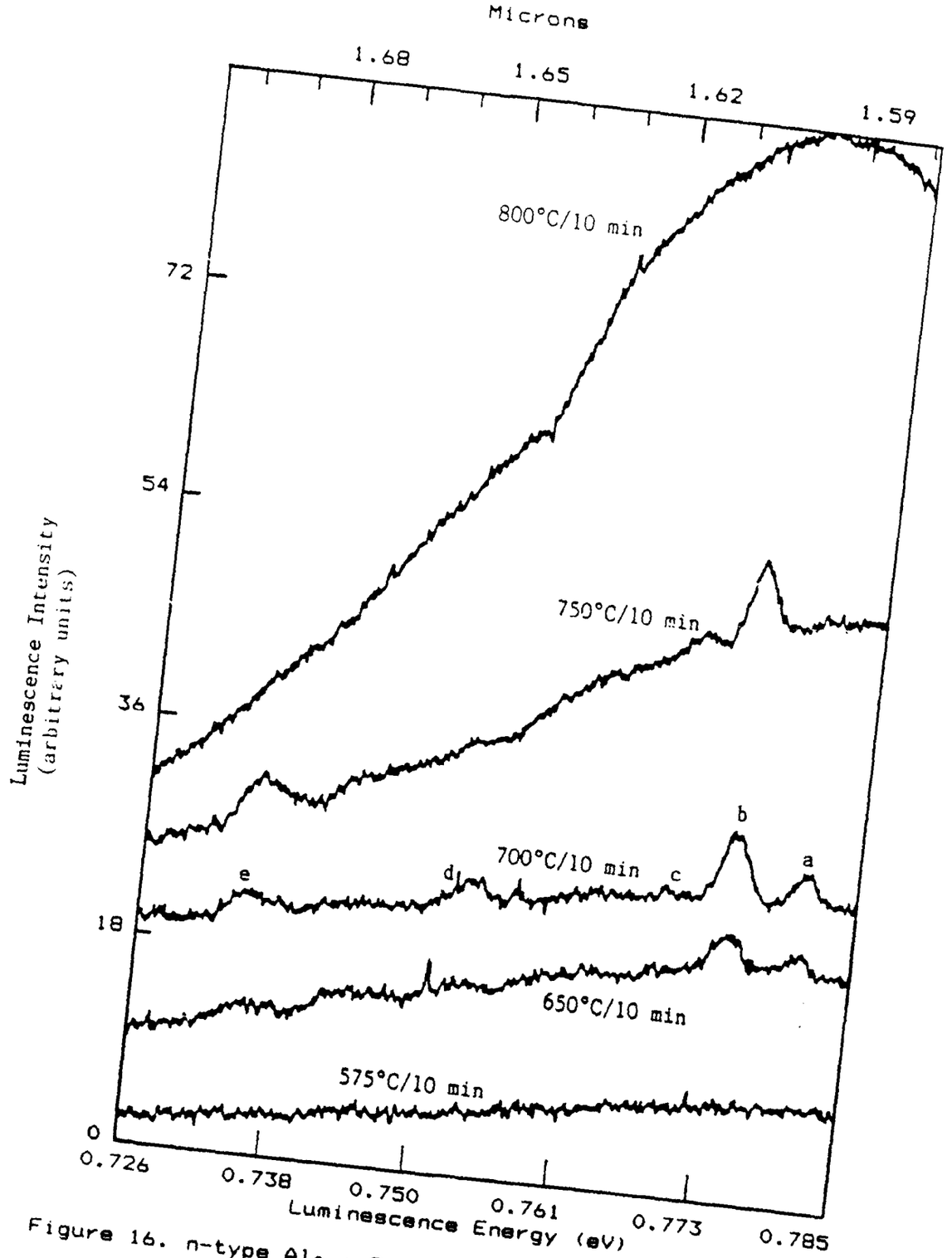

Figure 16. n-type $Al_{0.15}Ga_{0.85}As$:U Sample Spectra at Various Annealing Temperatures

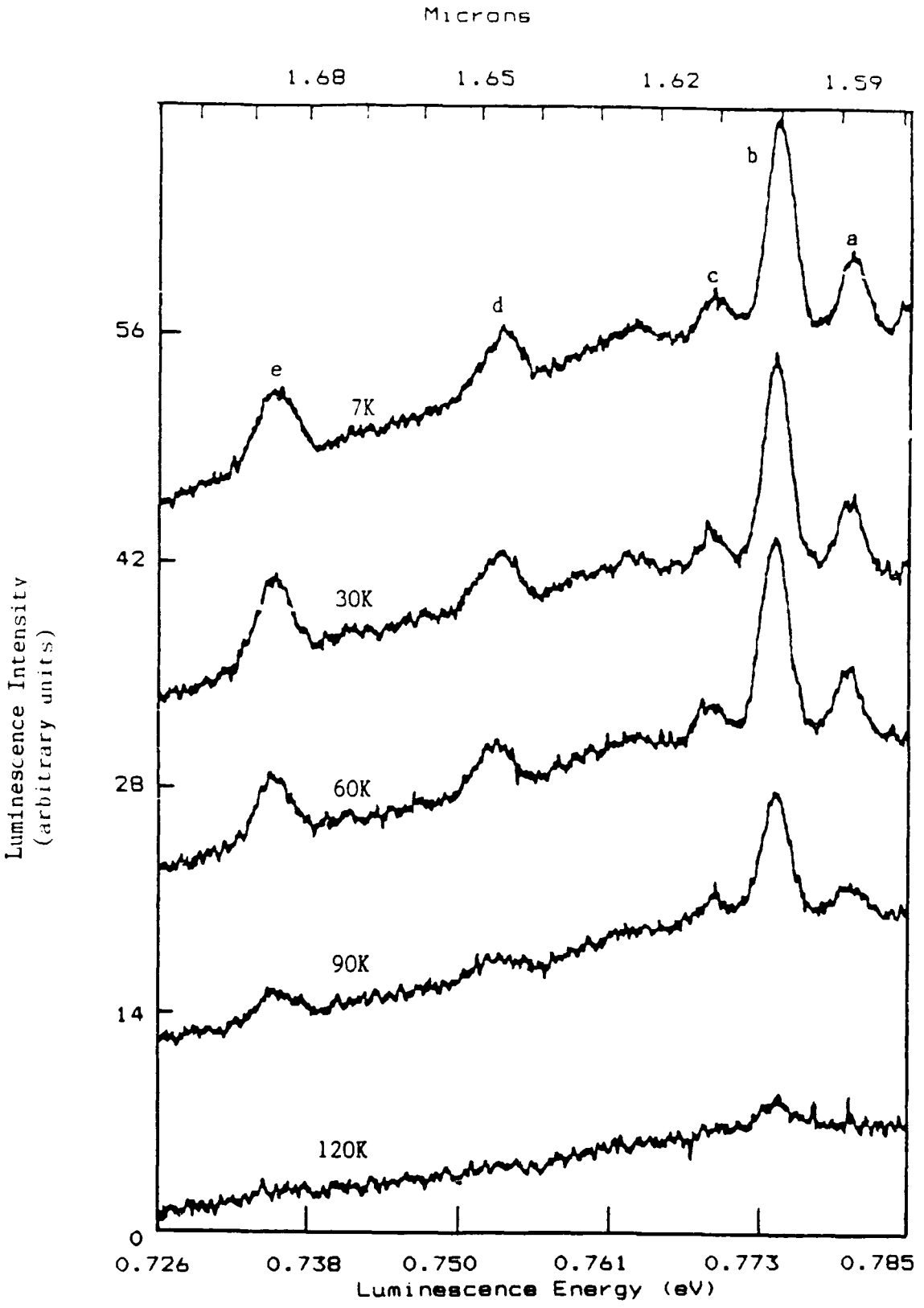

Figure 17. Thermal Quenching of n-type $Al_{0.15}Ga_{0.85}As$:U Spectra for the 700°C/10 min Annealed Sample

Each peak's intensity was equally quenched as the sample temperature was raised up to 120K. This indicates a common luminescence center for all the emissions. Thermal quenching did not become rapid until 90K. The strongest line at 1.60 microns was observed up to 120K.

From the increase in signal intensity with higher anneal temperatures, the center appears to be from a lattice site. Diminishing intensities at the high anneal temperature along with the development of a non-uranium related broad band indicates the breakdown of the crystal structure from the high anneal temperatures. The optimum annealing temperature for $Al_{0.15}Ga_{0.85}As$:U is 700°C. No thermal broadening occurred as the sample temperature was raised. Band edge emissions were not quenched with the addition of uranium. No other uranium emissions, either sharp or broad, were detected between 0.8 and 1.8 microns (the range of the germanium detector). In measuring the sample's luminescence (annealed at 700°C/10 min), no frequency shifts were observed in any of the uranium related signals as the sample temperature was raised from 7 to 120 K.

D. Comparison of Semiconductors

The samples studied can be classified into two groups: those with an arsenic ligand and those with a phosphorus ligand. The arsenic group is made up of SI-GaAs:U, n-type GaAs:U and n-type $Al_{0.15}Ga_{0.85}$:U. The phosphorus group contains SI-InP:U and n-type GaP:U.

All the arsenic semiconductors had the same five lines except

in n-type GaAs:U where only the two strongest were observable. This implies the same luminescence center for all three doped semiconductors. The uranium emissions are sensitive to the host's conductivity type as seen by the greatly reduced signals from n-type GaAs:U compared the those in SI-GaAs:U. The n-type $Al_{0.15}Ga_{0.85}As$:U sample also had a much reduced set of lines compared to the SI-GaAs:U sample. Figure 18 shows the results for the four semiconductors, n-type $Al_{0.15}Ga_{0.85}As$:U, SI-InP:U, SI-GaAs:U, and n-type GaAs:U, offset along the Y-axis. From this figure, the relative intensities of the uranium related signal can be seen. These spectra were made using the 647.1 krypton laser at 200 mW. Though less intense, the ternary semiconductor ($Al_{0.15}Ga_{0.85}As$:U) does however have the lower thermal quenching rate.

Of the two semiconductors in the phosphorus group, only the SI-InP:U sample had detectable uranium emissions. Once again the n-type conductivity seemed to hinder the radiative efficiency of the uranium ions.

The 1.67 micron line in the InP:U sample was the strongest of all five semiconductors. Since this line is not found in any of the other three emitting semiconductor types, one may not suspect a similar center. However this difference may only reflect the presence of different ligands in the crystal. If the radiative uranium centers are located at gallium or indium sites, then the ligands will be the nearest neighbors and will have the greatest influence on the amount of crystal field splitting of the uranium 5f energy levels.

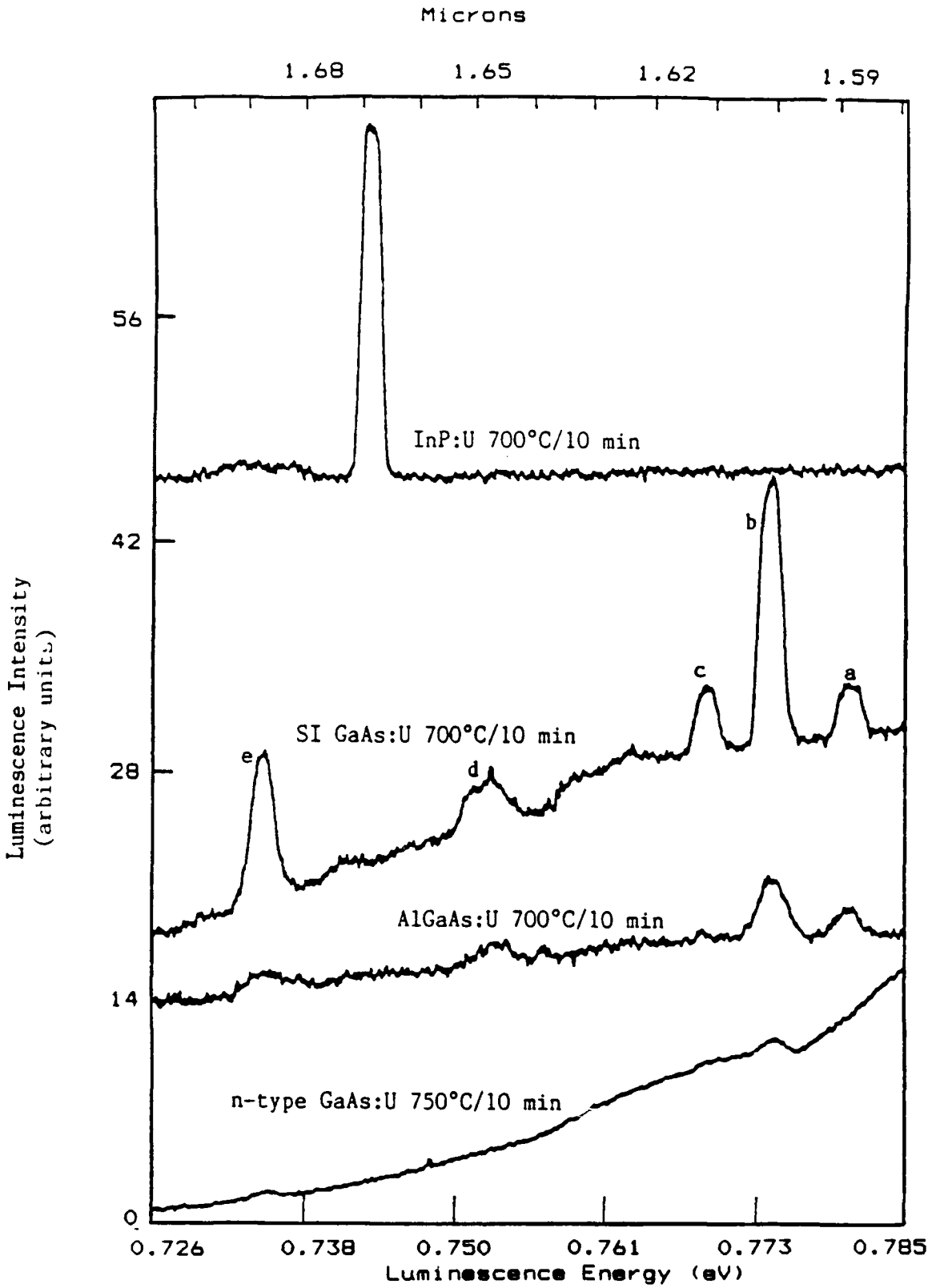

Figure 18. Intensity Comparison of Strongest Emitting Samples

None of the semiconductors showed any "hot" lines as the samples were studied with increased sample temperature. Also, all the uranium lines were relatively sharp. The InP:U band at 1.685 is probably composed of a few lines that were inseparable due to their weak intensities and the sensitivity limits of the equipment used in this study. Figure 19 shows the sharp uranium emissions of $Al_{0.15}Ga_{0.85}As$:U, SI GaAS:U and SI InP:U from 1.3 to 1.8 microns at a sample temperature of 7K. The broad bands that extend over the entire range of the uranium emissions are non-uranium related. Also, in this figure one can see the zero signal levels of the three spectra (extreme left of each spectrum).

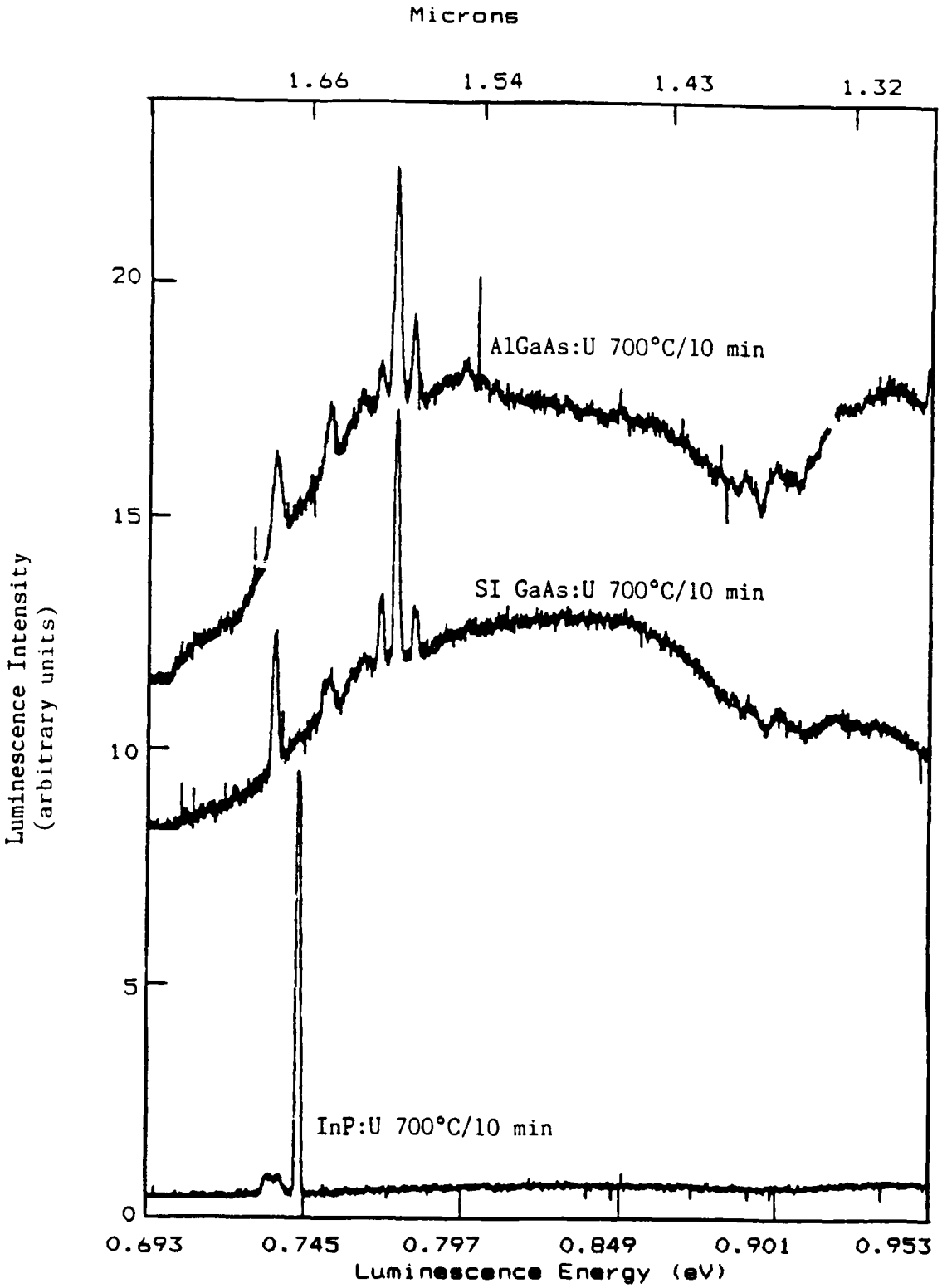

Figure 19. 1.3 to 1.8 micron Spectra of Uranium Doped Semiconductors at 7K

Chapter V

V. Conclusions and Suggestions for Future Study

The following statements can be made from this study of uranium doped III-V semiconductors and AlGaAs:

1. The optimum conventional furnace annealing temperatures using the proximity method for 10 minutes are:

   a) 700°C for SI-GaAs:U, $Al_{0.15}Ga_{0.85}As$:U, and SI-InP:U.

   b) 750°C for n-type GaAs:U.

2. One uranium luminescence center seems to be formed in SI-GaAs:U, $Al_{0.15}Ga_{0.85}As$:U, n-type GaAs:U.

3. One uranium luminescence center seems to be formed in SI-InP:U. The wavelengths of the uranium lines in InP:U did not coincide with any lines from the arsenic containing semiconductors. This may be due to the effect of the different ligand causing the splitting of the uranium 5f energy levels to be different.

4. Uranium signals were seen in AlGaAs:U and n-type GaAs:U for the first time.

5. The uranium emissions seem to be significantly effected by the host's conductivity. Semi-insulating semiconductors gave the strongest emissions.

6. The 1.59 line in SI-GaAs:U was seen for the first time as well as the weak 1.685 band in SI-InP:U.

7. The wavelengths of the uranium emissions from this study and information from past studies suggests that the ion state of the uranium is U^{4+}.

To gain a fuller understanding of uranium doped semiconductors, other studies need to be made. These include selective excitation luminescence, Zeeman spectroscopy, and lifetime measurements.

Theoretical calculations of U^{4+} energy levels also need to be made before definite assignments can be made to the uranium ion state and energy levels involved in the transitions.

The uranium signal in even the best samples studied were very weak. Experiments in co-doping and in varying the conductivity of samples may lead to greater radiative efficiencies. As their final uses will most likely be electrically driven, electrical measurements of these doped semiconductors need to be made. Such efforts may shed some light on the mechanisms involved in these materials. Also, other semiconductor groups should be examined such as II-VI and IV semiconductors. Lastly, other actinides such as neptunium, plutonium, and americium may be studied in semiconductors.

Bibliography

1. Colon, Capt J. E. Low Temperature Photoluminescence Study of Ytterbium Implanted Into III-V Semiconductors and AlGaAs. MS Thesis AFIT/GEP/89D. School of Engineering, Air Force Institute of Technology (AU), Wright-Patterson AFB Ohio, December 1988.
2. Pomrenke, Maj G. S. "Actinide Activated Luminescence in Uranium Implanted III-V Semiconductors," Journal of Applied Physics, (February 1990).
3. McKelvey, J. P., Solid State and Semiconductor Physics, Malabar, Robert E. Krieger Publishing Company, (1986).
4. Dexter, D. L., Excitons, New York, Interscience Publishers, (1965).
5. Pankove, J. I., Optical Processes in Semiconductors, New York, Dover Publishers, (1975).
6. Dean, P. J., "Photoluminescence as a Diagnostic of Semicon ductors", Prog. Crystal Growth Char., vol. 5, 89-175, (1982).
7. Yen, W. M., Laser Spectroscopy of Solids, Berlin, Springer-Verlag, (1981).
8. Edelstein, N. M., Lanthanide and Actinide Chemistry and Spectroscopy, Washington D. C., American Chemical Society, (1980).
9. Title, R. S., "Optical Spectra and Paramagnetic Resonance of U^{4+} Ions in Alkaline Earth Fluoride Lattices,Physical Review, vol 128, no. 1, 62-66, (1962).

10. Brown, I. G., "Multiply Stripped Ion Generation in the Metal Vapor Vacuum Arc", Journal of Applied Physics, vol. 63(10), 4889-4898, (1988).

Vita

Captain Michael B. Scott [redacted] He graduated from Great Mills High School in Great Mills, Maryland in 1978 and served two years in Anchorage, Alaska for the U.S. Air Force. In 1984, he graduated from Oklahoma State University with a Bachelor of Science degree in Physics.

After re-entering the service, he served as Data Acquisition and Weapons Analyst Officer for the B-1B FOT&E Test Team at Dyess AFB, Texas. In 1988, he entered the Air Force Institute of Technology at Wright-Patterson AFB, Ohio, to pursue a Master of Science degree in Engineering Physics.

[redacted]

SECURITY CLASSIFICATION OF THIS PAGE

REPORT DOCUMENTATION PAGE

Form Approved
OMB No. 0704-0188

1a. REPORT SECURITY CLASSIFICATION UNCLASSIFIED	1b. RESTRICTIVE MARKINGS
2a. SECURITY CLASSIFICATION AUTHORITY	3. DISTRIBUTION/AVAILABILITY OF REPORT Approved for public release; distribution unlimited
2b. DECLASSIFICATION/DOWNGRADING SCHEDULE	
4. PERFORMING ORGANIZATION REPORT NUMBER(S) AFIT/GEP/ENP/89D-9	5. MONITORING ORGANIZATION REPORT NUMBER(S)
6a. NAME OF PERFORMING ORGANIZATION School of Engineering 6b. OFFICE SYMBOL (*If applicable*) AFIT/ENP	7a. NAME OF MONITORING ORGANIZATION
6c. ADDRESS (*City, State, and ZIP Code*) Air Force Institute of Technology Wright-Patterson AFB OH 45433-6583	7b. ADDRESS (*City, State, and ZIP Code*)
8a. NAME OF FUNDING/SPONSORING ORGANIZATION 8b. OFFICE SYMBOL (*If applicable*)	9. PROCUREMENT INSTRUMENT IDENTIFICATION NUMBER
8c. ADDRESS (*City, State, and ZIP Code*)	10. SOURCE OF FUNDING NUMBERS PROGRAM ELEMENT NO. / PROJECT NO. / TASK NO / WORK UNIT ACCESSION NO
11. TITLE (*Include Security Classification*) Low Temperature Photoluminescence Study of Uranium Implanted into III-V Semiconductors and AlGaAs	
12. PERSONAL AUTHOR(S) Scott, Michael Buryl	
13a. TYPE OF REPORT MS Thesis 13b. TIME COVERED FROM _____ TO _____	14. DATE OF REPORT (*Year, Month, Day*) 1989 December 4 15. PAGE COUNT 55
16. SUPPLEMENTARY NOTATION	
17. COSATI CODES FIELD / GROUP / SUB-GROUP	18. SUBJECT TERMS (*Continue on reverse if necessary and identify by block number*) Photoluminescence Uranium III-V Semiconductor AlGaAs

19. ABSTRACT (*Continue on reverse if necessary and identify by block number*)

Thesis Advisor: Dr. Y. K. Yeo
Associate Professor of Engineering Physics

20. DISTRIBUTION/AVAILABILITY OF ABSTRACT ☒ UNCLASSIFIED/UNLIMITED ☐ SAME AS RPT ☐ DTIC USERS	21. ABSTRACT SECURITY CLASSIFICATION UNCLASSIFIED
22a. NAME OF RESPONSIBLE INDIVIDUAL Dr. Y. K. Yeo	22b. TELEPHONE (*Include Area Code*) (513) 255-2012 22c. OFFICE SYMBOL AFIT/ENP

DD Form 1473, JUN 86 *Previous editions are obsolete.* SECURITY CLASSIFICATION OF THIS PAGE

Abstract Uranium implanted into III-V semiconductors gives rise to relatively sharp emissions between 1.58 and 1.69 microns. The implantation was performed at a mean ion energy of 131 keV and a dosage of 4×10^{13} cm^{-2} using a high current metal ion source. The 5f-emissions were observed in semi-insulating (SI) GaAs, n-type GaAs, SI-InP, and $Al_{0.15}Ga_{0.85}As$ with the strongest emission from SI-GaAs. Conventional annealing established a $700^{o}C$ and 10 minute optimum anneal condition for most of the samples. The 5f-emissions may be observed up to a sample temperature of 120K.